

RESEARCH ON DIGITAL
TRANSDUCER PRINCIPLES
SECOND SEMIANNUAL REPORT

for the
NATIONAL AERONAUTICS AND SPACE ADMINISTRATION
GRANT NGR-44-012-043

Covering the Period
July 1, 1967 - December 31, 1967

by
William H. Hartwig
Project Director

The University of Texas at Austin
Austin, Texas 78712

TABLE OF CONTENTS

ABSTRACT	iv
I. PREFACE	1
II. METAL-INSULATOR-SILICON "TUNNELING" DIGITAL DEVICES	2
A. INTRODUCTION	2
B. THEORETICAL CONSIDERATIONS	3
C. EXPERIMENTS PERFORMED	5
D. EXPERIMENTAL RESULTS	11
E. SUMMARY	18
III. CHEMICAL VAPOR DEPOSITION	20
A. INTRODUCTION	20
B. FILM DEPOSITION	20
C. FILM PROPERTIES	24
D. OTHER RECENT WORK	25
E. ELLIPSOMETER EVALUATIONS	26
F. FUTURE WORK IN CVD	26
IV. POLYMER DIELECTRIC INVESTIGATION	29
A. INTRODUCTION	29
B. FREQUENCY DEPENDENCE OF POLYMER DIELECTRICS	29
1. Description of Experiment	
a. Fabrication	
b. Measurement	
2. Experimental Results on Numerous Samples	
a. capacitance vs frequency, Typical Sample	

b.	Dissipation Factor vs Frequency, Typical Sample	
c.	Percent Capacitance Change vs Frequency, Many Samples	
C.	AGING CHARACTERISTICS OF POLYMER DIELECTRICS	37
1.	Description of Experiment	
a.	Aging Set-up	
b.	Measurement	
2.	Experimental Results on Cross-Type Samples	
a.	Capacity vs Time	
b.	Dissipation Factor vs Time	
3.	Experimental Results on Three-Point Samples	
a.	Capacity vs Time	
b.	Dissipation Factor vs Time	
4.	Percent Capacity Change vs Thickness vs Time	
D.	ANALYSIS OF EXPERIMENTAL RESULTS	43
V.	OPTICAL DIGITAL TRANSDUCER CONCEPTS	45
A.	FREE-ELECTRON MODEL	45
B.	TRAPPED-CARRIER MODEL	47
C.	PHOTODIELECTRIC DIGITAL TRANSDUCER	49
D.	BIBLIOGRAPHY	50
VI.	NEW DIGITAL DATA STORAGE PRINCIPLE	56
VII.	ATTENDANCE AT MEETINGS, PAPERS, PUBLICATIONS	61

ABSTRACT

The first 18 months of work on NGR-44-012-043, Research on Digital Transducer Principles, has produced a number of practical digital transducer concepts and has seen the initiation of several new lines of research which clearly are new contributions to instrumentation. Previous reports described successful digital transducer for measuring temperature or magnetic field in a cryogenic environment. New principles using thin-film phenomena compatible with silicon integrated-circuit technology have been reported on. A deeper understanding of metal-polymer-silicon structures is seen in this volume. In particular, the necessary materials properties for the sharp discontinuity in conductivity of MPS devices are described. The polymer itself has been more exhaustively studied and its role in development of digital MIS transducers is discussed.

Additional progress has been made in exotic dielectrics to use as active transducer material in MIS structures. Titanium dioxide has been successfully deposited from a chemical vapor. This is one more step from passive dielectrics, such as Si_3N_4 reported in Vol. IV of the First Annual Report, to a material which can alter the charge transport by response to an external stimulus. Properties of titanium dioxide films are given as the results of preliminary measurements.

Two new areas of digital transducer behavior are reported in some detail. Previously the photodielectric effect was described in silicon and germanium as a basis for optically tuning a resonant cavity. The transducer accepts light intensity as the analog input and produces a frequency change as a digital response. The bandwidth of that detector is above a megacycle. During the period of this report a parallel study on silver-doped cadmium-sulphide revealed a new kind of photodielectric

response which produces a frequency change proportional to the integral of light intensity. A frequency change of about 1.2 KHz per minute for a continuous 4800 Å light approximately 1 microwatt in intensity was observed in an 825 MHz cavity. This effect is shown to be applicable at other wavelengths with suitable selection of materials. The infinite lifetime of the trapped carriers is a disadvantage which can be overcome by mechanical vibration or selecting materials with shallower traps such as aluminum.

The second new area of digital behavior is elaborated on for the first time in this report. A recent development by Dr. D. I. Tchernev on digital information storage at JPL is being continued at The University of Texas under his direction. Magnetic thin films of MnBi have been shown capable of storing magnetic bits which are less than one micron in diameter. Writing is done by a laser. We will propose to provide partial support to this work in the future.

Each phase of this research program is being examined to determine future emphasis, particularly in response to specific NASA requirements.

I. PREFACE

The program of research is a search for discontinuous or digital behavior in nature which could be exploited in the design of a new class of transducers. This concept is clearly a bold one. No great assurance could have been given at the beginning that what had not been found previously by others would now be discovered.

It has become apparent, however, that such phenomena exist. Considerable ingenuity is often required to bring about the proper circumstances, and much hard work must still be done to get consistent results. None-the-less, several completely feasible digital transducers have already been described.

This report comes at the three-quarter point in the grant period. It reflects continuing progress along several fruitful paths. Only a fraction of the useful ideas have been pursued to a logical conclusion. The current work being reported here is in a state of active research. Much has reached the development of technology, and the rest is in various stages of emergence from a sound concept to a practical device. A renewal proposal for steps funding will be submitted prior to the Final Report.

II. METAL-INSULATOR-SILICON "TUNNELING" DIGITAL DEVICES

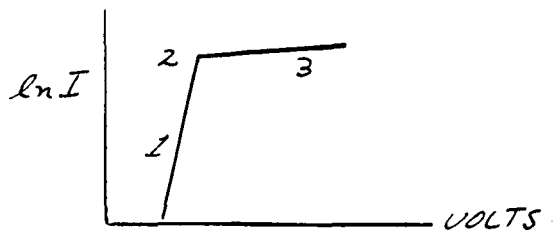
Previous reports have described in some detail a proposed digital transducer using electron transport phenomenon between a metal and a semiconductor separated by a very thin polymer insulator. Since tunneling is the dominant mechanism for only the thinnest films, the designation MIS "Tunneling" Digital Devices is only a convenient one. The theory explaining this non-linear current in a metal-insulator-semiconductor (MIS) sample was proposed by Wilmsen. The salient points of this theory that pertain to the immediate development of the device are recalled in a following section. Subsequent work, reported in Vols. I, II and III of the First Annual Report explored in some detail the non-linear current mechanism between two metal plates separated by a very thin polymer insulator. Although this work was done with metal-insulators-metal samples (MIM) the electron transport mechanisms are identical with those in an MIS device. Additionally, it allowed a more detailed investigation of thin polymer film technology to be pursued.

Although successful MIS samples had been constructed by Wilmsen in his work mentioned earlier it was felt that in order to assure accurate and consistent results in the present effort a certain amount of work had to be done on the MIS device technology since it differs appreciably from that used to fabricate MIM junctions. A large portion of the work done during this report period was oriented toward this end and will be reported below.

A number of MIS samples were constructed during this period, the exact nature of the sample depending on the extent of the technological development. The experimental data from these samples will be summarized and analyzed at the end of this report.

B. THEORETICAL CONSIDERATIONS

The proposed digital transducer is based on the performance of an MIS junction when an external bias is applied. The V-I characteristic, as reported previously, can be expressed, somewhat ideally, by the curve below:



As can be seen, the current through the device increases exponentially with the applied bias up to a certain point and then becomes roughly independent of the voltage applied. If the polarity of the bias is reversed, no saturation is seen and the current continues to increase exponentially with bias. Put quite simply, the saturation effect depends upon the formation of a depletion layer in the surface states adjacent to the insulator. For N type semiconductor this depletion layer is formed by applying the positive bias to the semiconductor and the negative to the field plate. For P type materials the opposite polarity will achieve the same effect. Reversing the polarity for either type of material will not only create a depletion region but will flood the surface states with mobile majority carriers making the semiconductor appear "metal-like" and cause the sample to display characteristics similar to MIM devices.

The reverse bias characteristics, as sketched above, may be broken into three regions. The first region, 1, is characterized by an exponential increase in current with applied bias. In this region, the semiconductor depletion region has not yet formed and the device performance is that of an MIM sample. The slope of this region is determined solely by the insulator thickness, the specific electron transport mechanism at work and certain constants of the insulator itself. The slope may also be a slight function of age and electrical stress as was previously observed and reported.

The second region or knee of the curve is actually the onset of the depletion region. The rate at which the slope changes from a "vertical" to a "horizontal" value is a function of the rate of exhaustion of the surface states and the underlying bulk state.

The third region corresponds to the depletion layer growth. The slope in this region is inversely proportional to the depletion growth rate. The slope will be "flat" if the depletion layer grows as least as fast as the bias is increased across the sample since the electric field across the insulator will remain constant. If the bulk state density is comparable to the surface state density and both are fairly large then the slope in this region will be large and the saturation effect will not be pronounced.

In order to make an effective device, the sample should have characteristics that can be associated with the three operating regions mentioned above. Initially, the current should rise rapidly with an increase in bias. A factor of ten increase in the current with less than $1/2$ volt increase in bias seems quite possible. This slope can be achieved by using a sufficiently thin insulator, i.e., one less than 100 \AA so that the natural log of the current will be proportional to the applied bias rather than the square root of the bias. It will then be required that, once the depletion region begins to form, it will grow rapidly. A rapid growth of the depletion layer will cause the current to switch from an exponential increase with bias to an function independent of bias. This transistion region will be minimal if the surface properties quickly give way to the bulk properties and if the two are markedly different. Ultimately, the resolution of the device will depend on what range of bias it takes to increase the current by an appreciable factor and then switch the device into the saturation mode. Once saturation has been achieved, the current through the sample should be as independent of the bias as possible. This can be achieved only if the

sample is lacking in charge sites caused either by impurity doping or mechanical imperfections.

Thus, it was felt that the present research effort should be centered around these requirements:

1. The insulator must be approximately 100 \AA thick. It would be desirable to decrease this thickness even further but the failure rate due to insulator imperfection increases rapidly.

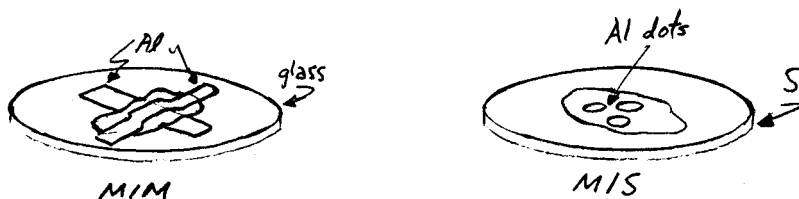
2. The surface state density of the semiconductor must be markedly higher than that of the bulk and kept localized at the surface. This quantity may be controlled by varying the method of surface preparation such as using mechanical rather than chemical polish or vice-versa, the surface state density for a mechanically polished sample being appreciable higher than that for a chemical polished sample.

3. The mobile and local charge density in the bulk of the material should be low. High resistivity silicon with a low mechanical defect density must be used.

C. EXPERIMENTS PERFORMED

Extensive work has already been performed on the polymer dielectric to be used with the MIS devices and a portion of the results have been included in a previous report. These experiments employed the polymer as an insulator in simple metal-insulator-metal capacitors. This configuration involved two strips of evaporated aluminum in the form of a cross and separated where they intersect by the polymer. The whole device was built on a glass slide shown in the figure below. Contact was made with the capacitor electrodes at these extremities by bearing down on them with screws from a sample holder. No contact problem were ever encountered because of the positive method with which they were made. It is obvious, however, that any MIS devices require a completely different configuration. The semiconductor wafer re-

places both the substrate and the bottom electrode as shown in the figure and hence, the top electrode cannot overlap the insulator and extend onto the semiconductor itself or a short circuit will occur.



In effect, the top electrodes are required to "float" on the insulator. This precludes a direct pressure contact with them because of the delicate nature of the supporting insulator. Thus, methods for making positive contact to this top electrode and the backside of the silicon substrate had to be devised.

A series of experiments were conducted with the above MIS configuration to establish a means of contact with the top metal electrode which, initially, was evaporated aluminum. Bringing a metal probe directly down on the field plates proved fruitless in all attempts, demonstrating the fragility of the insulator. It was felt that whatever did actually contact the electrode would have to do so with a minimum of force and spread whatever force it did exert evenly over the entire metal plate. In order to achieve this, a small "blob" of GaIn eutectic (in this case a liquid slush at room temperature) was attached to the tip of the metal probe and the probe brought near the electrode so that only the "blob" would touch it. Theoretically, the field plate would respond to the light even pressure of the blob by making contact and, in turn, the blob would make contact to the test probe. A number of experiments using aluminum electrodes over insulators of moderate thickness ($\sim 150 \text{ \AA}$) showed that this was not always the case. In the large majority of cases physical contact to the electrode could be made without puncturing the insulator

however, the electrode contact made was always intermittent and data which was directly dependent on the quality of the electrical contact was unreproducible. When the blob was withdrawn from the aluminum surface little or no trace of the eutectic could be seen to remain. It was concluded that the GaIn did not wet the surface of the aluminum for one reason or another and, that in order to obtain good electrical contact, wetting action would have to take place.

A third group of samples were made using gold, silver, tin, lead, and nickel top electrodes. Several interesting pieces of data came out of this experimentation and the results need further analysis. The majority of samples made with gold electrodes proved to be good but the GaIn eutectic attacked the gold vigorously and when the probe was lifted, the remaining gold was lifted away. This process gave rise to electrical characteristics which were erratic and unsuitable. The large majority of samples made with the other metals (silver, tin, lead, and nickel) yielded short circuits. The GaIn blob made good electrical contact to these metals as witnesses by surface wetting but in almost every case, the sample was shorted. To insure that the failures were a function of the metal used and not a function of the blob contact an additional group of samples were made in the cross configuration in which contact could be made without disturbing the insulator at all. In each of these cases the results were again negative, i.e., the samples were all shorted. Between attempts with the different metals a number of samples were made with aluminum electrodes (in both the "cross" and "dot" configuration) and in each case the samples measured good. Hence, it was felt that the high incidents of short circuits was a function of the electrode metal used and not of the configuration or contact method.

On a number of different basis, it would appear that this phenomena mentioned above has no obvious, logical explanation. All of the metals used had boiling points

near that of aluminum so that the impact energy of vaporized metal atoms arriving at the insulator would be roughly constant. If one would expect that the "replicating" metals, characterized by low atomic mobilities, would tend to fill in pinholes and microfissures and thereby cause shorts, then it would seem that aluminum would yield poor results and gold and silver would give the best yields. This, of course, was not found to be true. Hence, it would seem that the only immediate explanation is that aluminum is a "slow diffuser" in the polymer insulator while the others assume a "faster" or more active role.

At this point in the effort it seemed readily obvious from a standpoint of device yield, that aluminum was the necessary choice for electrode material. The problem became to achieve good electrical contact between the GaIn blob and the aluminum electrode. The problem was solved by adding another step in the fabrication process. A new evaporation mask was cut and silver dots, smaller in diameter than the aluminum dots, were laid over the aluminum electrodes. This additional step was performed immediately after the aluminum dots were evaporated without removing the sample from the vacuum so that intimate contact was assured between the aluminum and silver. With this configuration, aluminum was contiguous to the polymer and assured a high sample yield while silver was exposed in order to make good contact with the GaIn blob. A group of samples made and tested in this way showed a good yield and repeatable electrical characteristics.

It is obvious, that any practical device cannot utilize such a delicate arrangement as described above. Research will have to be done to ascertain the optimum method for bonding contacts to the top electrodes or a totally different configuration will have to be employed.

Earlier research on relatively thin (100 \AA) MIM junctions showed that the

device yield was an extremely sensitive function of surface smoothness and preparation. On a number of occasions good ground glass substrates proved to be too rough to support a successful device. For this reason much thought was given to the preparation of the silicon surface to minimize sample failure due to surface irregularities. During the present research period commercially prepared silicon of both P and N type in the moderately low resistivity range ($\sim 10\Omega\text{cm}$) was available for experimentation. These wafers had been mechanically and chemically polished and, upon inspection, were found to possess high quality surfaces. Another group of wafers of N type silicon in the $100\text{--}500\Omega\text{cm}$ range were prepared in the lab. Some time was expended lapping and polishing these samples and, in general, the results were disappointing. Most wafers had suffered some work hardening at the surface and, when chemically polished, proved to be fairly pitted when examined under a $100\times$ microscope. The samples which were mechanically polished but not chemically etched appeared to have better surfaces than their chemically polished counterparts. At this point it was felt that building successful MIS devices on any of these high resistivity samples would prove to be a matter of luck.

It was felt that much of the inconsistency in the data from the early samples was due to poor contacts to the back side of the semiconductor substrates. Any rectification at this junction would seriously affect the V-I characteristics and mask any depletion effects at the insulator-semiconductor interface. Some attention was given to the problem of assuring that the back side contact to semiconductors substrate was ohmic. Such a contact can be made by several methods. They are:

1. a) For an N type semiconductor, use a metal with a smaller work function than the semiconductor itself ($\sim 4\text{eV}$ for Si); and for P type use a metal with a larger work function.

- b. While obeying criterion (a) also choose the metal so that if it were to be used as a dopant, it would enter N type material as a donor; for p type, use a metal which would enter as an acceptor.

2. Dope the semiconductor in the immediate vicinity of the contact location to the point of degeneracy. Most metals will then form an ohmic contact to this region.

The second method suggests that the ease with which an ohmic contact is formed is in some way proportioned to the doping density. This was observed with the samples ranging in resistivity from 10Ω cm. to 500Ω cm.; the lower resistivity material was fairly easy to contact while the high resistivity proved especially difficult. In all cases, the silicon was processed through a standard cleaning cycle which immediately preceded any attempt at making contact (boiling trichloroethylene degrease, boiling nitric acid strip, de-ionized water rinse, hydrofluoric acid oxide strip, de-ionized water rinse, methanol rinse, final clean in boiling trichloroethylene vapors.)

Three specific methods were attempted to make ohmic contact to the silicon substrates ranging from 10Ω cm. to 500Ω cm. These methods were described briefly below with observed results.

1. A simple evaporated coating of aluminum was deposited on N type Si and silver on P type. This method proved successful with the 10Ω cm. samples and little rectification was observed but showed only limited success with the medium and high resistivity materials.

2. A layer of nickel was first deposited on an N type sample in a standard electroless plating process. The sample was then heated to about 500°C for 1/2 hour. It was believed that the baking process would diffuse some of the phosphorous, an

inevitable impurity of the Ni, into the semiconductor a small distance and provide a basis for ohmic contact. The oxide on the Ni coating was then removed and a second application of Ni was made. This process provided good electrical contact to both 10 Ω cm and 500 Ω cm samples.

3. A thin layer of GaIn eutectic was spread on the back side of the N type samples immediately after the surface cleaning procedure. Fair contact was made to the 10 Ω cm and 100 Ω cm material but only poor contact was made with the 500 Ω cm samples. It was found that the quality of the contacts could be greatly improved if a solid piece of the eutectic (a slush at room temperature, composed of both liquid and solid phases) was first used to rub or scratch the Si surface and then a layer of the liquid portion "painted" on.

D. EXPERIMENTAL RESULTS

For the most part, the experimental results during this period may be divided into two groups (1) those technological steps necessary to fabricate and test successful devices, (2) data gleaned from testing completed devices. The previous sections contain most of the findings concerning the device technology. This section will concern itself with data gathered from the samples themselves. Almost all of the samples which yielded data were, in one way or another, compromises with what was described previously as perhaps the ideal sample. Representative of this data are the results from five samples included below.

Figure #1 shows the characteristics of a sample built on P type, 10 cm. mechanically polished, Si with an evaporated Ag back electrode, Al and Ag top electrode and a 120 \AA insulator. Saturation is observed in the reverse bias configuration, however the current through the device is unusually high for a 120 \AA insulator and capacitance measurements were accompanied by a very high dissipation factor ($\sim .5$). Subsequent

attempts to reproduce the above data with several other samples built in exactly the same way failed in that saturation was never seen.

Figure #2. This sample was built on 10Ω cm, N type mechanically polished Si with a Ni plated backside contact, Al and Ag top electrode and a $150 \overset{\circ}{\text{A}}$ insulator. As can be seen, the two bias polarities are somewhat symmetric and no saturation is seen in the reverse direction. The slope of the characteristic is rather shallow owing to the thickness of the insulator. The dissipation factor of the device is moderately low (~ 0.05). It is a possibility that the low dissipation factor may be the result of a better insulator or backside contact than the sample in figure 1.

Figure 3 and 4 show the data from two different samples fabricated in identical ways. Both samples differ from the one described immediately above in that these had evaporated Al back electrodes rather than plated Ni contacts. The current shows some tendency to saturate in the reverse direction and, in figure 4, it is seen that when the reverse bias characteristics were rerun a more pronounced tendency to saturate was observed. This "forming" characteristics of the sample was previously observed with MIM samples and represents some "memory" capability of the polymer. Both samples had dissipation factors which were intermediate between those of the samples in figure 1 and figure 2. (Sample figure 3, ~ 0.07 ; sample figure 4, ~ 0.3). Once again, it is uncertain whether a correlation exists between the dissipation factor and the quality of the insulator or the quality of the insulator or the quality of the contact or both.

Figure 5. This data was taken from a sample built on 500Ω cm. N type mechanically polished Si. The backside contact was made by the Ni plating method and appeared to be quite good. The data taken was extremely erratic and provides at best, trends. It will be noticed however, that these currents began to saturate almost immediately when the reverse bias was applied and, even in the forward direction, the current increased only sluggishly with voltage. The insulator thickness was roughly $150 \overset{\circ}{\text{A}}$ and cannot be completely responsible for the shallow slope. It is possible that the characteristic,

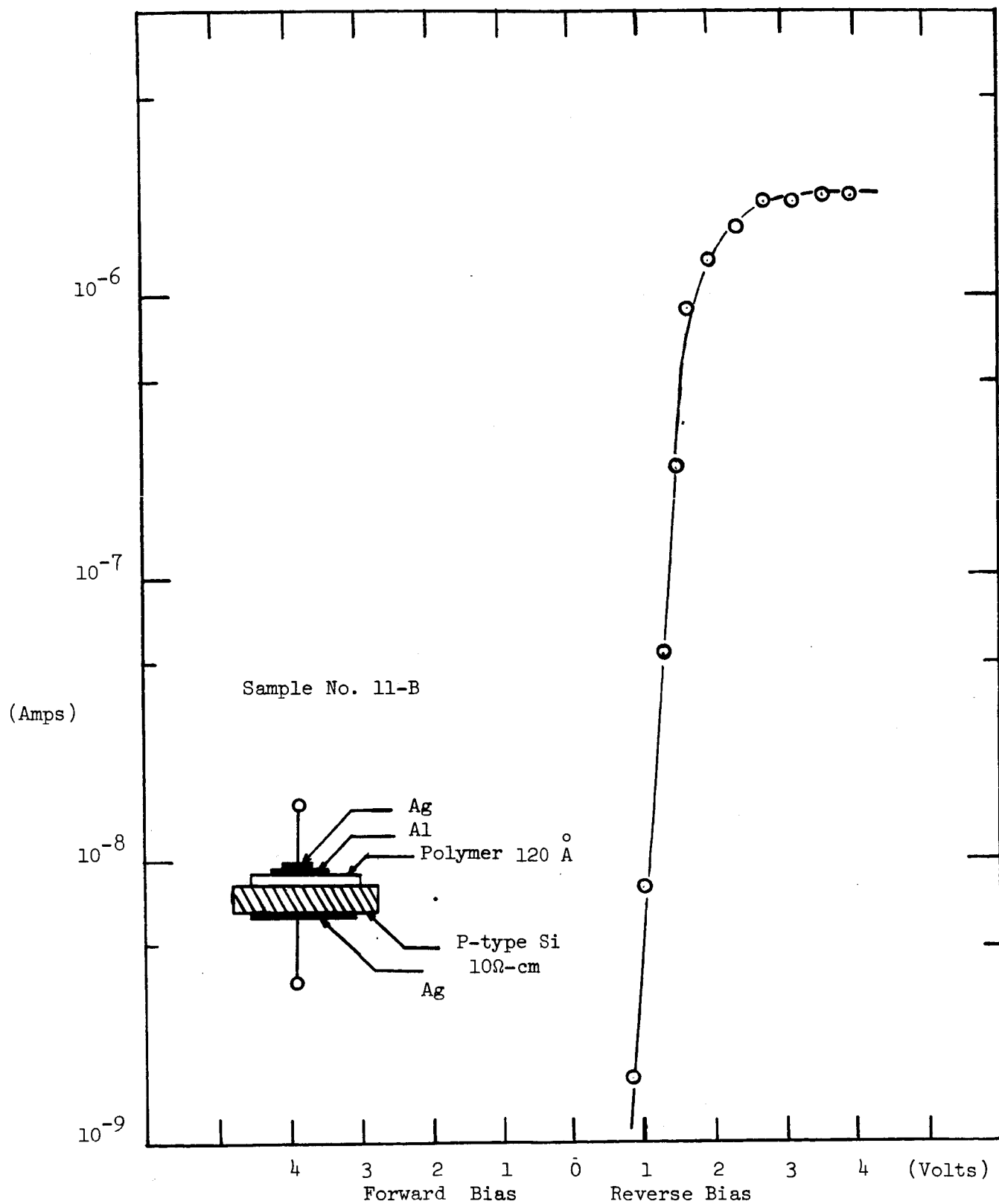


Figure 1

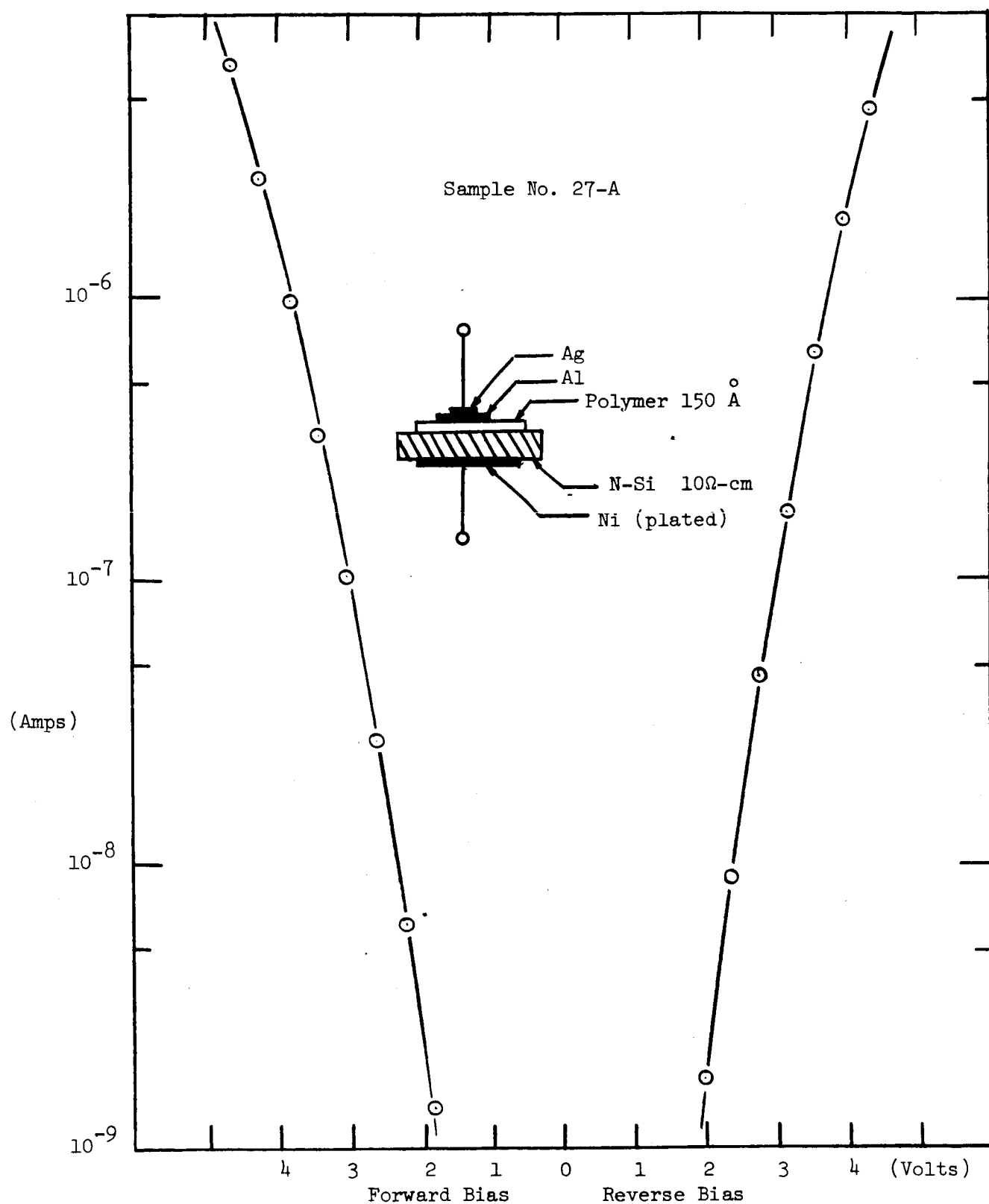


Figure 2

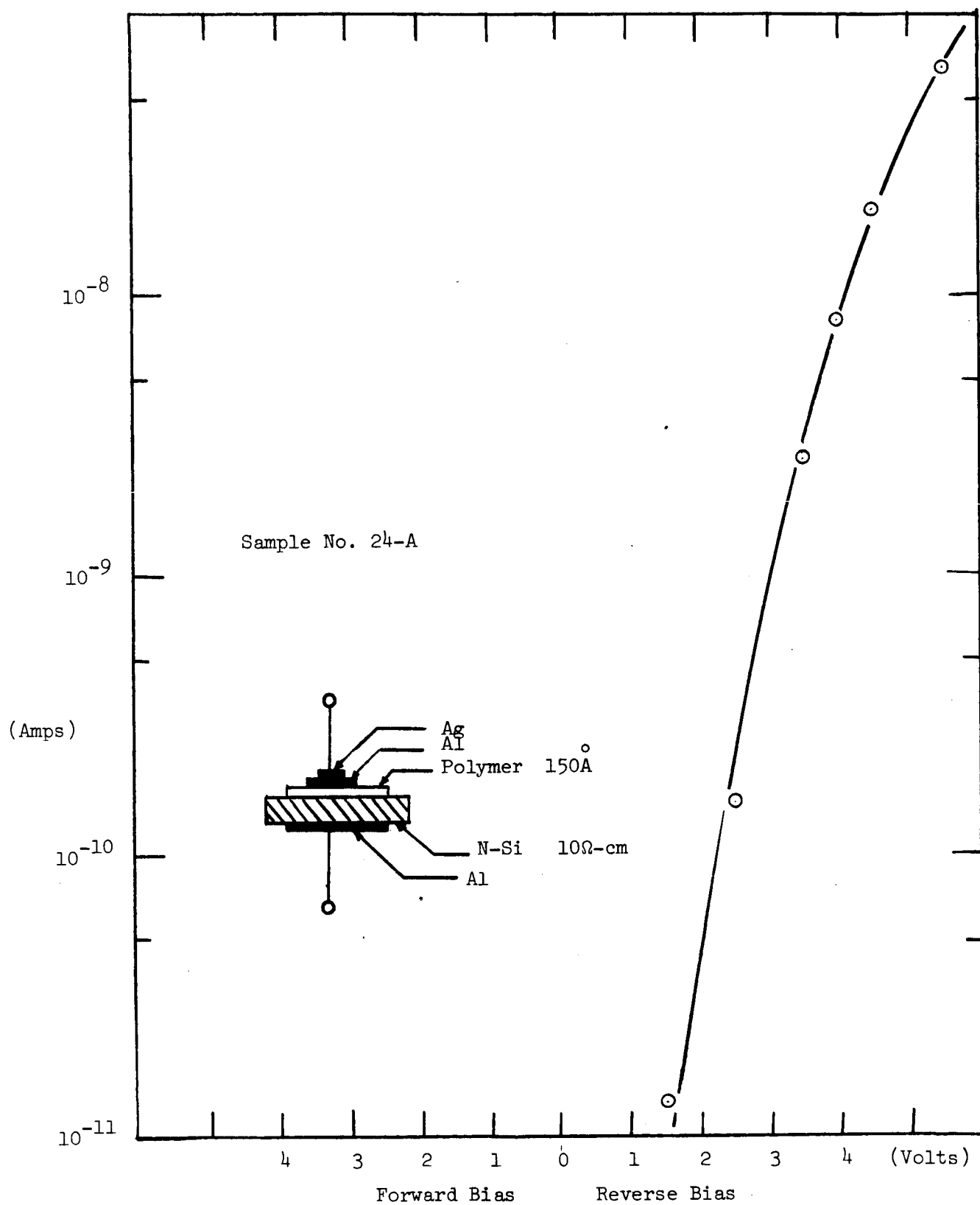


Figure 3

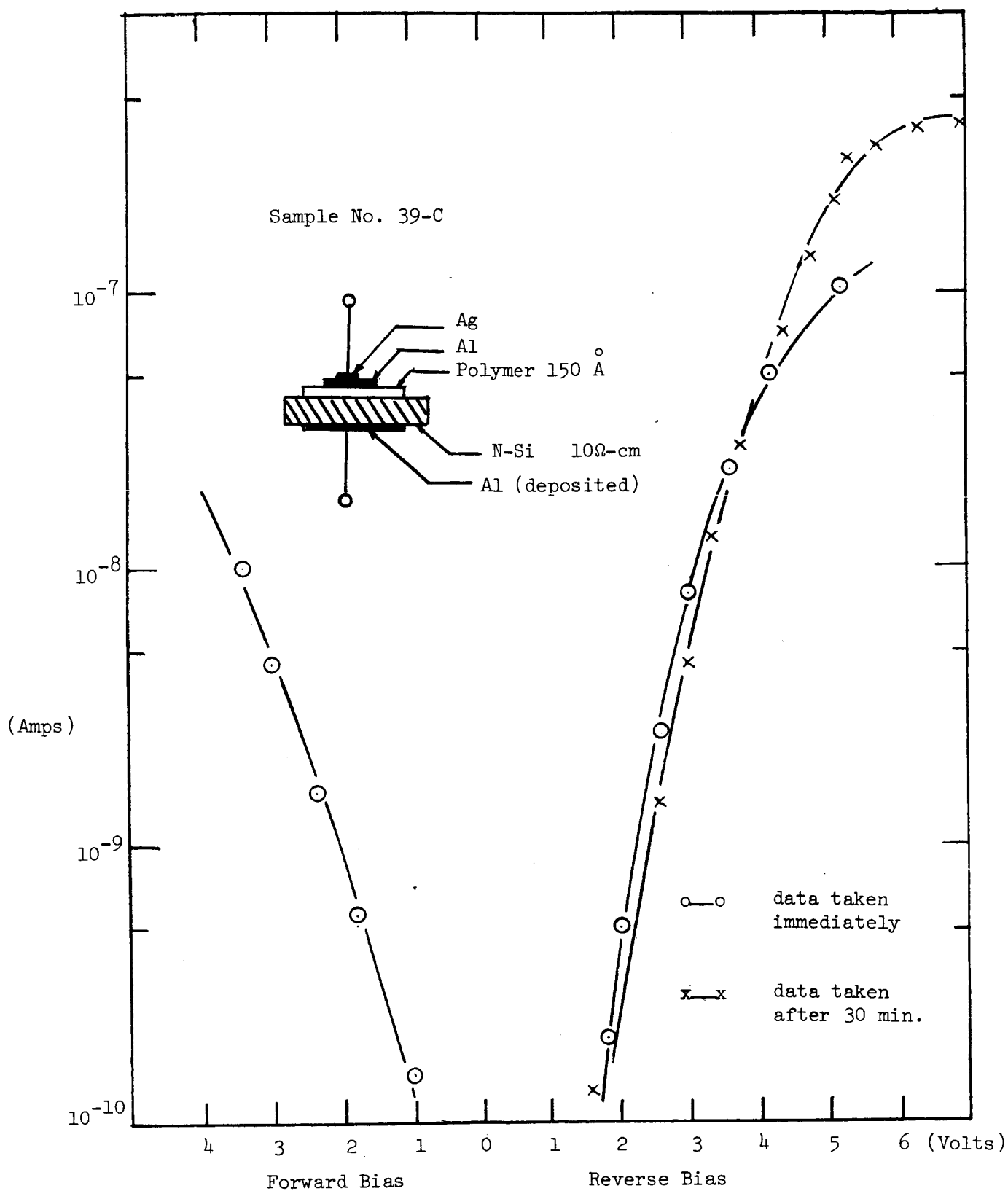


Figure 4

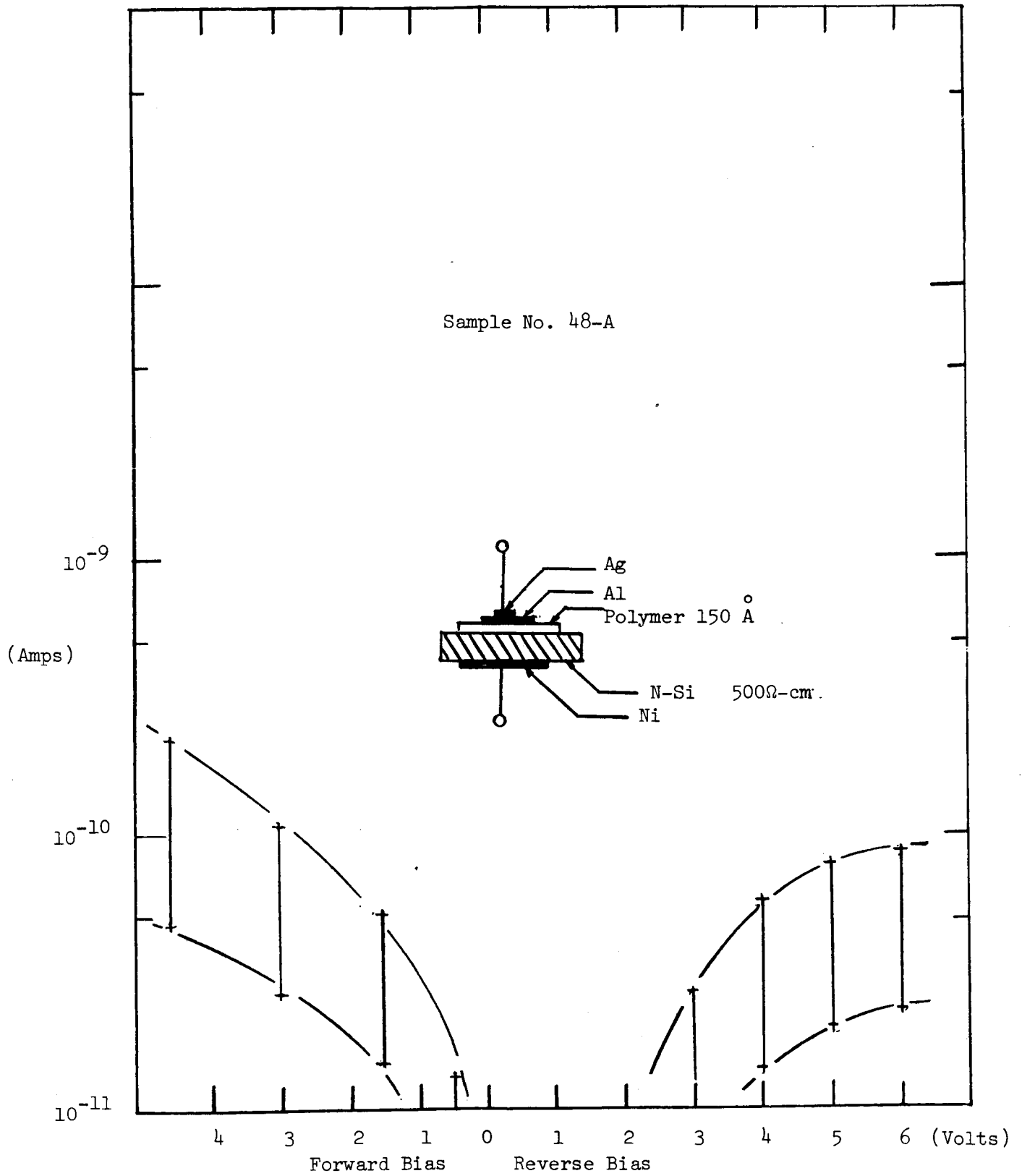


Figure 5

at least in the reverse direction, can be explained by the immediate onset of a depletion layer.

A minimum number of conclusions can be drawn from this data without the benefit of further experimentation.

1) The slope of the V-I characteristics at low bias levels in either polarity was generally predictably shallow due to the thickness of the insulator (150 \AA). This portion of the slope could be steepened by decreasing the film thickness.

2) No saturation effect was observed in the "forward" bias configuration. This was an expected result.

3) The majority of samples showed only a weak tendency to saturate in the "reverse" direction and the saturation took the form of a gradual decreasing dependency of current on voltage, not a sharp break where the current through the device is independent of the applied bias. Since $10 \Omega \text{ cm.}$, mechanically polished Si substrates were used, it is felt that the surface state density was sufficiently high to prevent the formation of an extensive depletion region within the range of bias that could be put on the device.

4) Two samples showed saturation as predicted by theory. The difference between the performance of these and that of the majority of samples could be due to a difference in the wafer surface preparation, the quality of the electrode contact to the semiconductor, the insulator or any of a number of factors.

• E. SUMMARY

Early analysis of some recent data not included in this report, add some order to the seemingly confused facts presented above. It would appear that the $10 \Omega \text{ cm.}$ sample in figure 2 and the $500 \Omega \text{ cm.}$ sample in figure 5 are representative of possible

limiting cases. That is, the surface state density of the 10Ω cm. mechanically polished samples is high enough to prevent the establishment of a depletion region before the critical breakdown field of the insulator is reached while the surface state density of the 500Ω cm. material is small enough to cause the formation of a depletion layer almost immediately upon application of the bias. This most recent work indicated that samples fabricated on N type, $80-120\Omega$ cm. Si with GaIn backside contacts saturated to various degrees and with various sharpnesses in the reverse bias condition. Work is presently being carried out to construct and test samples of this type and to determine how to optimize the desired V-I characteristics.

Much of the progress reported here has to do with techniques which are proprietary and not readily available in the literature. The second six months will have time scheduled for a re-examination of available sources of information to provide as many new guidelines as can be made available.

III. CHEMICAL VAPOR DEPOSITION

A. INTRODUCTION

The development of methods for the chemical vapor deposition of uniform and stable thin films of dielectrics with a wide range of characteristic, especially high dielectric constants, is the objective of this phase of the program. Dielectric materials may function in several roles in digital devices. The purpose of investigating them is to find classes of behavior which are compatible to tunneling digital transducers by having a characteristic response to an external stimulus.

The report covering the period from January 1 to June 30, 1967 dealt into a theoretical development of chemical vapor deposition. The report discusses basic kinetic considerations, vapor plating requirements, a proposed deposition apparatus, the advantages of chemical vapor deposition, and thermodynamics considerations which lead to the determination of the optimum operating conditions and provide a powerful tool for analyzing new chemical transport processes.

B. FILM DEPOSITION

During this period a considerable amount has been accomplished in going from the previous theoretical treatment to the current stage of growing dielectric films. The system described in the previous report was designed and built. Figure 6 shows the experimental system. The graphite susceptor was coated with silicon nitride to prevent the graphite from decomposing when heated. The temperature sensor is an infrared radiation pyrometer which is focused through a quartz window onto the substrate surface. An rf induction coil surrounding the quartz deposition chamber heats the graphite susceptor. The rf generator is a 1 kw, 300 kHz unit which required critical initial tuning in order to obtain coupling to heat the susceptor to the required temperature. However, this generator is now matched to where it will heat the susceptor to 1100°C

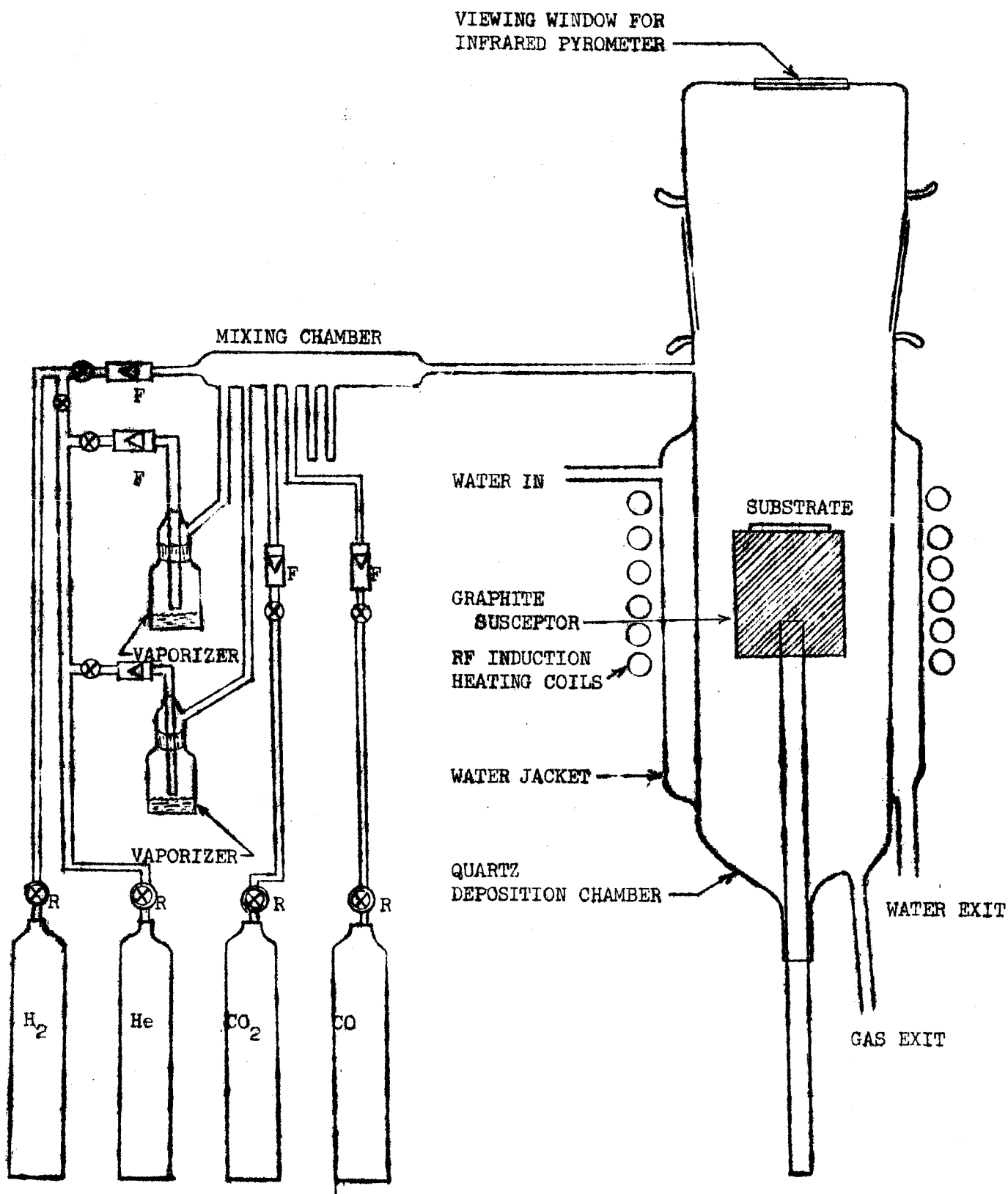
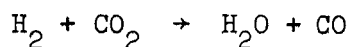


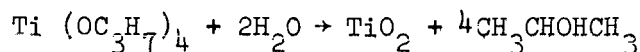
FIGURE 6 DEPOSITION APPARATUS

or better. The water jacket surrounding the reaction chamber keeps the quartz wall temperature low enough to limit deposition to the susceptor substrate. Pressure regulators, regulating valves, and flow meters provide the necessary regulation and control. A gas washing bottle serves as the vaporizer for the reactant, tetraisopropyl titanate, which is a liquid at room temperature.

Current work in the laboratory has concentrated on using hydrogen gas, carbon dioxide gas, and an organometallic, tetraisopropyl titanate. The reactions are:



and



The thin dielectric film is deposited on a platinum coated quartz substrate. The polished quartz discs (1 inch diameter x 1/16 inch thick) are cleaned in a potassium dichromate and sulfuric acid glass cleaning solution. They are then rinsed several times in deionized water, rinsed in methanol, boiled in trichlorethylene, and then stored in trichlor. The platinum is then evaporated onto the quartz in the vacuum system at 10^{-5} torr pressure. The sample is then placed in the deposition chamber. The system is then flushed out with 2 l/min of He gas for several minutes. The sample is heated to the desired temperature and the gases are introduced. The parameters in use at the present time are:

H_2 : 538 cc/min

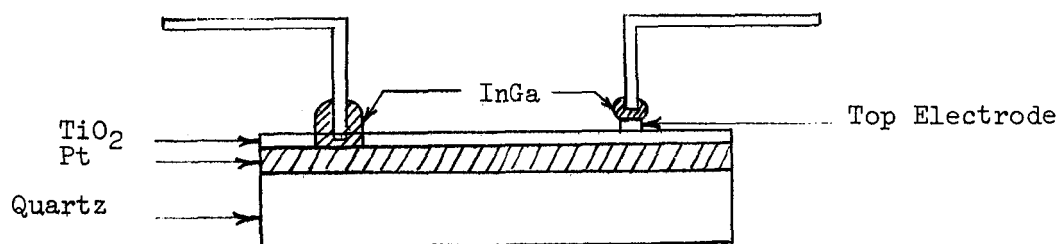
CO_2 : 243 cc/min

He across $\text{Ti} (\text{OC}_3\text{H}_7)_4$: 4600 cc/min

Temperature of $\text{Ti} (\text{OC}_3\text{H}_7)_4$: 100°C

Temperature of substrate : 850°C

The thickness of the film is determined approximately from the interference colors which are observed on the sample as the film grows. Films approximately 2000 Å thick are grown in about 30 minutes with the above conditions. The sample is now ready for the deposition of the upper metal electrode. Evaporated aluminum dots were used for this purpose at first. However, considerable difficulty was experienced in making contact to the Al dot. Success was achieved by evaporating a small silver dot on top of the Al dot. Then the probe with a dot of InGa paste can be lowered onto the sample. The InGa wets the Ag and makes good contact to it. The InGa would not wet the Al alone. Contact is made to the bottom Pt electrode by scratching through the insulator. Sketch below shows this arrangement.



Method of Making Contacts to MIM Devices

Some problems have been encountered in the film growth process. One of these problems is that of obtaining an even growth rate across the surface of the sample. At first the gases tended to flow down the walls of the chamber and a "dead spot" was formed at the center of the sample where the growth rate was retarded. The system was modified and the gases directed toward this spot, but then the growth was faster at the center than at the edges. This has been corrected somewhat but additional work needs to be done toward obtaining a uniform growth rate across the entire sample. Another problem is that of system contamination. After several samples have been made a white powdery deposit forms on the walls of the reaction chamber and to some

extent in the mixing chamber and some of the gas lines. If this is not removed periodically, the resulting samples exhibit poor electrical properties. This deposit is easily removed by rinsing with a weak solution of hydrofluoric acid and deionized water.

C. FILM PROPERTIES

The evaluation of the film properties is still at an early stage. Many of the problems which have hampered work in this area, such as uneven growth, system contamination and making contact to the top electrode, have been overcome and the program is just at the beginning stages of getting reproducible sample data on the film properties. The area of the top electrode varies from .79 to .93 mm² depending on the mask used. The thickness of the samples tested ranged from 1200 to 2100 angstroms. The capacitance per unit area is about 2.0 $\mu\text{f}/\text{in}^2$. The dielectric constant ranged from 40 to 60 for most of the samples tested. The dissipation factor measured at 1 kHz ranged from 6% to 15% with the average near 10%. The breakdown strength is disappointing so far with most samples breaking down at under 2 volts. It is believed that the reason for this may be that the TiO_2 is non-stoichiometric. The TiO_2 may be oxygen deficient in which case it would exhibit some semiconducting properties. This can be overcome by heating in oxygen atmosphere to build up the oxygen in the film. If this is found to be the case then the reactant concentrations will be changed to add more oxygen to the mixture. This procedure is to be tried immediately. At 1.5 vdc the leakage current was 1.6×10^{-11} amps giving a dc leakage resistance of 0.94×10^{11} ohms. Martin¹ reports the following values for amorphous TiO_x : dielectric constant, 90; dissipation factor, 2.6%; breakdown voltage, 10V; capacitance per unit, $1.0 \mu\text{f}/\text{in}^2$; dc leakage resistance, 1.67×10^{11} ohms. The above were measured at 1 kc and for

thickness of 2500 Å. These films were formed by a glow discharge technique. Feuersanger² reports values for TiO_2 prepared from TiCl_4 as: dielectric constant, 80; specific capacitance, $0.5 \mu\text{f}/\text{cm}^2$; dissipation factor, 2.3%; and leakage current of $7.7 \times 10^{-10} \text{ amp}/\text{cm}^2$ at a field of $3.5 \times 10^3 \text{ v}/\text{cm}$. These films were about 1500 Å thick. Lakshmanan³ reports capacitance of $.30 \mu\text{f}/\text{cm}^2$ and dissipation factors of 5.5% at 1 kc for TiO_2 films between 1000 and 1600 Å thick formed by reactive sputtering. The breakdown voltage was between 2 and 10V. The dc resistance were between 10^9 and 10^{10} ohms.

From the above comparisons one can see that the values obtained in our laboratory are comparable to films formed elsewhere by other techniques. The fact that our numbers represent a beginning attempt on a small number of samples certainly shows promise that our films might well surpass those of other workers when our optimum conditions are found.

D . OTHER RECENT WORK IN CVD

Considerable effort has been shown recently by other workers in CVD. In September, 1967, the Materials Science and Technology Division of the American Nuclear Society and the Vapo-Metallurgy Committee of the Metallurgical Society of the AIME sponsored a conference on chemical vapor deposition. The papers presented are in book form.⁴ They include papers on the theory of deposition, methods of deposition, and applications and evaluation. In November the Air Force Materials Laboratory and the University of Dayton sponsored an international symposium on decomposition of organometallic compounds to refractory ceramics, metals, and metal alloys. The Fall 1968 meeting of the Electrochemical Society will include a symposium on new methods of forming dielectric thin films.

E . ELLIPSOMETER EVALUATIONS

Anticipated difficulty in etching the TiO_2 coupled with the fact that this is a destructive process eliminated multiple beam interferometry for thickness measurements. The method of ellipsometry which is non-destructive and capable of extremely high accuracy will be used for evaluating the thickness and refractive index of the films produced in this program. Work during this period involved becoming acquainted with the techniques of ellipsometry, calibrating the Gaertner ellipsometer, and writing a computer program which would analyze the reflected light beginning with the fundamental equation governing ellipsometry, the law of reflection, Snell's law of refraction, and Fresnel's reflection and transmission coefficients. The method of ellipsometry essentially consists of reflecting a beam of elliptically polarized light off the surface in question and measuring the polarization properties of the reflected beam. Among other things, the polarization properties of the reflected beam depend on the thickness of any absorbed layer on the surface. The computer program, written by H. G. Rylander, III, determines the thickness and the complex index of refraction of thin dielectric films coating metallic substrates. The computer program has just recently been put in final form and the accuracy of it and the alignment of the ellipsometer have been checked by putting in data from McCrackin⁵ and data measured for several SiO_2 films of various thickness on Si. The program and the ellipsometer are now ready to be used to evaluate the thickness and refractive index of thin dielectric films.

F. FUTURE WORK IN CVD

There are several things which will be done in the immediate future in this work. The first of these will be to oxidize the TiO_2 films and vary the deposition parameters in an attempt to obtain a stoichiometric film and a film which exhibits better electrical

properties. Chemical analysis data will be taken to determine the exact composition of the film. The electron probe or neutron irradiation techniques will be used for this. When better films are obtained then more electrical data must be taken to study the conduction mechanisms and dielectric properties of these films.

BIBLIOGRAPHY

1. Martin, H. B. "Development of Microelectronic Circuits for Linear Applications." AD 287 650, October, 1962
2. Feuersanger, A. E. "TiO₂ Dielectric Films Prepared by Vapor Reaction," Proc. IEEE, December, 1964, Page 1463-65
3. Lakshmanam, T. K. "Chemical Formation of Microcircuit Elements" AD 613563, March, 1965
4. Schaffhauser, A. C. Proceedings of the Conference on Chemical Vapor Deposition of Refractory Metals, Compounds, And Alloys, September, 1967
5. McCrackin, F. L., et al, "Measurement of the Thickness and Refractive Index of Very Thin Films and the Optical Properties of Surfaces by Ellipsometry" J. of Research, A. Phys and Chem, Vol. 67A, July-August, 1963, pp 363-77

IV. POLYMER DIELECTRIC INVESTIGATION

A. INTRODUCTION

The value of polymer thin films as insulating materials in MIS structures have been great enough to justify an systematic investigation of the characteristics which are important to the project. This has lead to development of a technique for growing reproducible films with controlled thickness, measurement of capacity and dissipation factor as a function of frequency, and measurement of these parameters with aging. This section of the report covers the measurement of these properties and some preliminary analysis of the results.

B FREQUENCY DEPENDENCE OF POLYMER DIELECTRICS

1. Description of Experiment

a. Fabrication

Metal-Polymer-Metal capacitors are formed by polymerizing silicone diffusion-pump oil vapors on a metal substrate and evaporating a metal film top electrode after the film was grown to the desired thickness. The details are described in Vols I and III of the First Annual Report. Both crossed-strips and three-dot configurations are used. The attachment of electrodes to isolate dots has proved more damaging to the polymer than when contact is made at the ends of the crossed strips.

b. Measurement

A general Radio Capacitance-Measuring Assembly Type 1620-A was used to measure the capacitance and the dissipation factor of the samples. The bridge is designed to cover a frequency range from 20Hz to 20 KHz

continuously and two steps for 50 KHz and 100 KHz. It covers a capacitance range of 10 pf to a maximum of $1\mu\text{f}$ without any external standard capacitor. The dissipation factor from 1 PPM to 1 may be read directly at 1 KHz with an accuracy of $\pm(0.1\% + 10 \text{ PPM})$. The samples are put in a shield case and co-axial cables used to connect the sample to the bridge. The cables were kept as short as possible to reduce lead capacitance, even though, the lead capacitance was still significant, it was measured to be 8 pf and was subtracted from the indicated capacitances.

On all measurements, the input signal was kept at 0.1V to assure the field more to order of magnitude below breakdown level and consequently, measurements have been possible without any chance whatever of incident breakdown or ionization phenomena. The constant input signal voltage also prevented the reading from errors due to the change of voltage, because the capacitance is voltage dependent. All samples are measured in air. Therefore it is required to measure the samples immediately after being taken out from the vacuum system and finish in shortest period to avoid the possible variation due to aging effect.

The bridge measures the capacitance, C_p , and dissipation factor, D , of an effective parallel combination of capacitance and resistance. No correction is necessary for analyzing the sample in parallel equivalent model.

2. Experimental Results on Numerous Samples

Over 100 samples have been made to refine the technique and get enough data to establish trends.

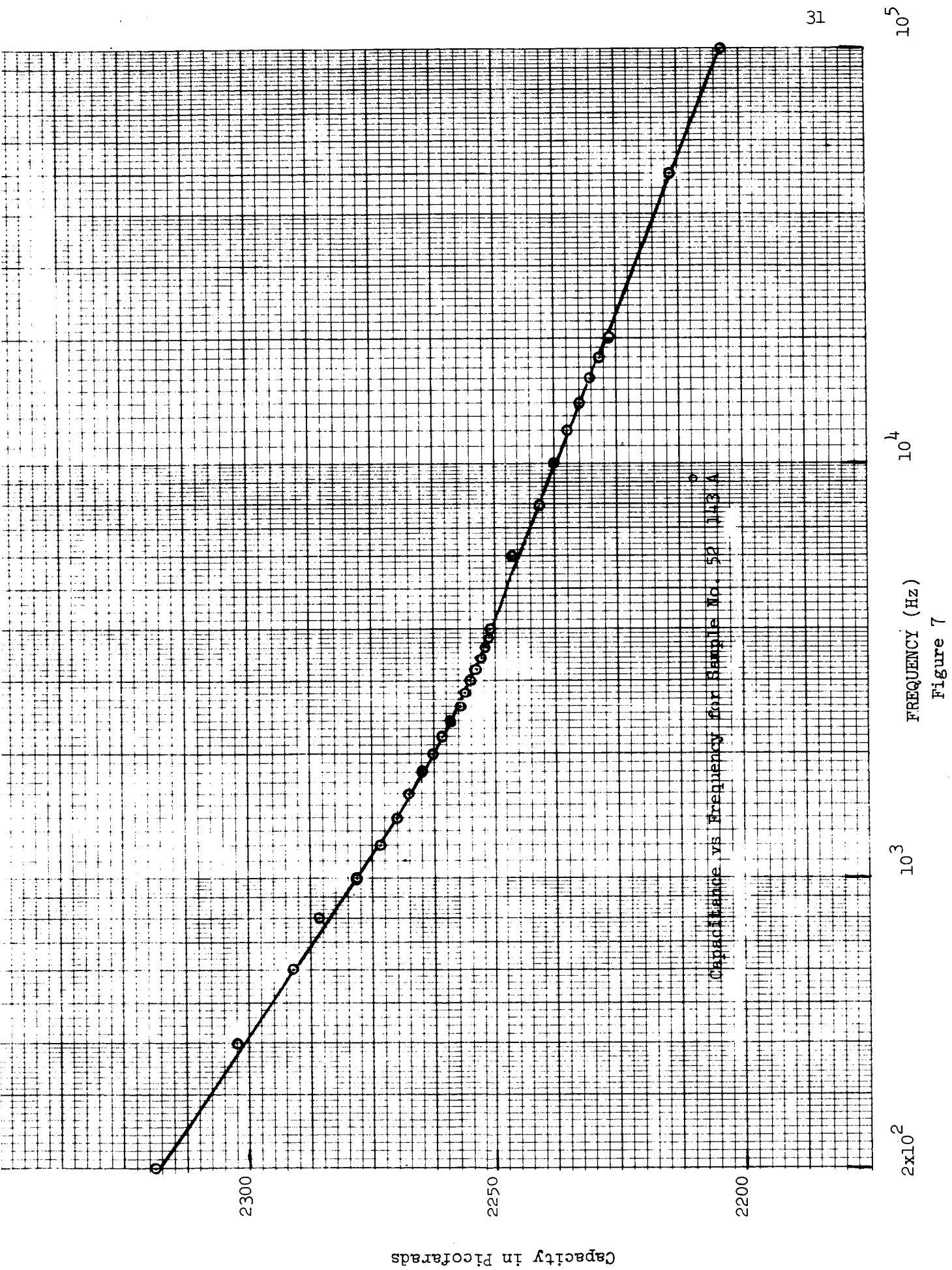


Figure 7

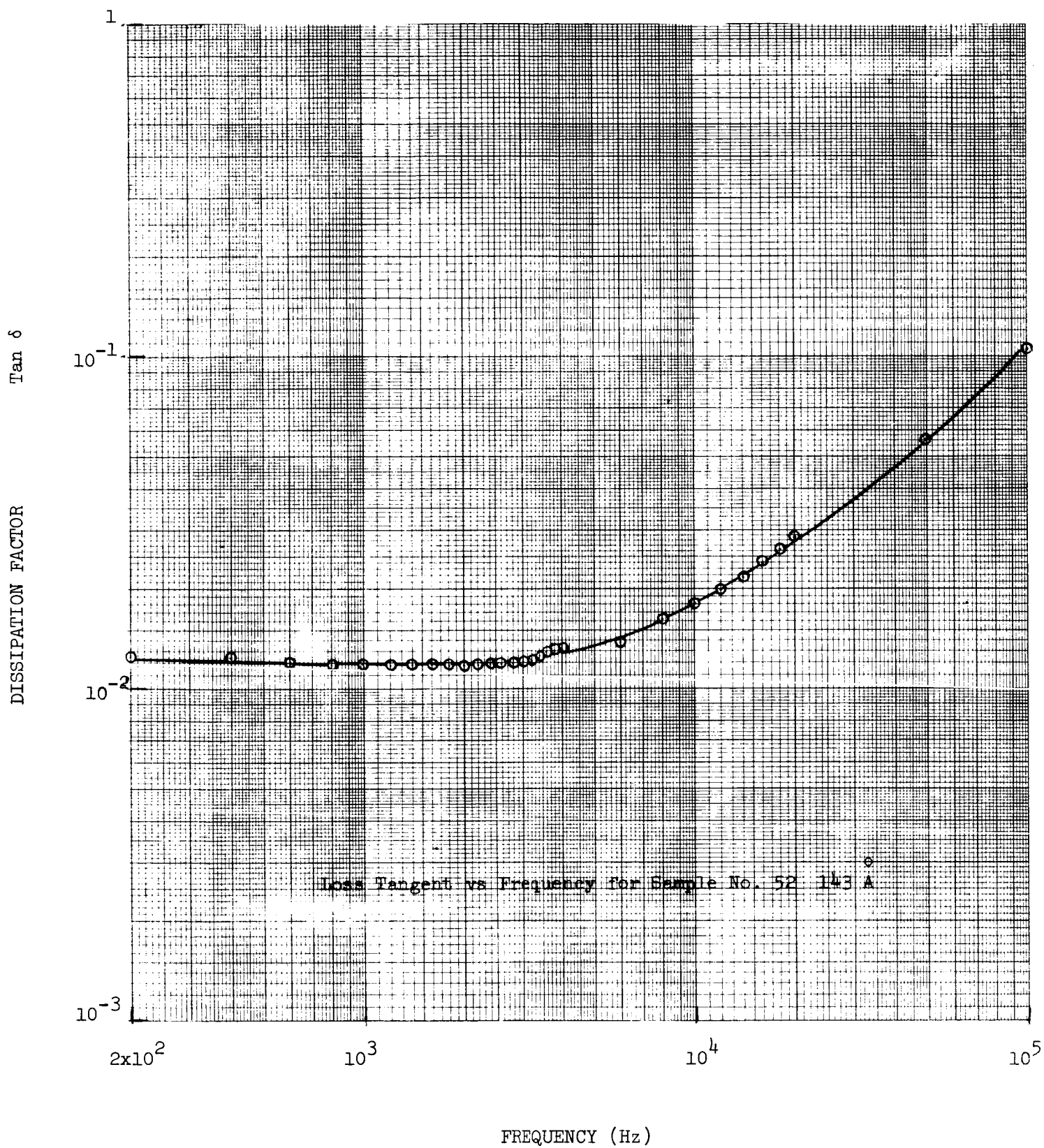


Figure 8

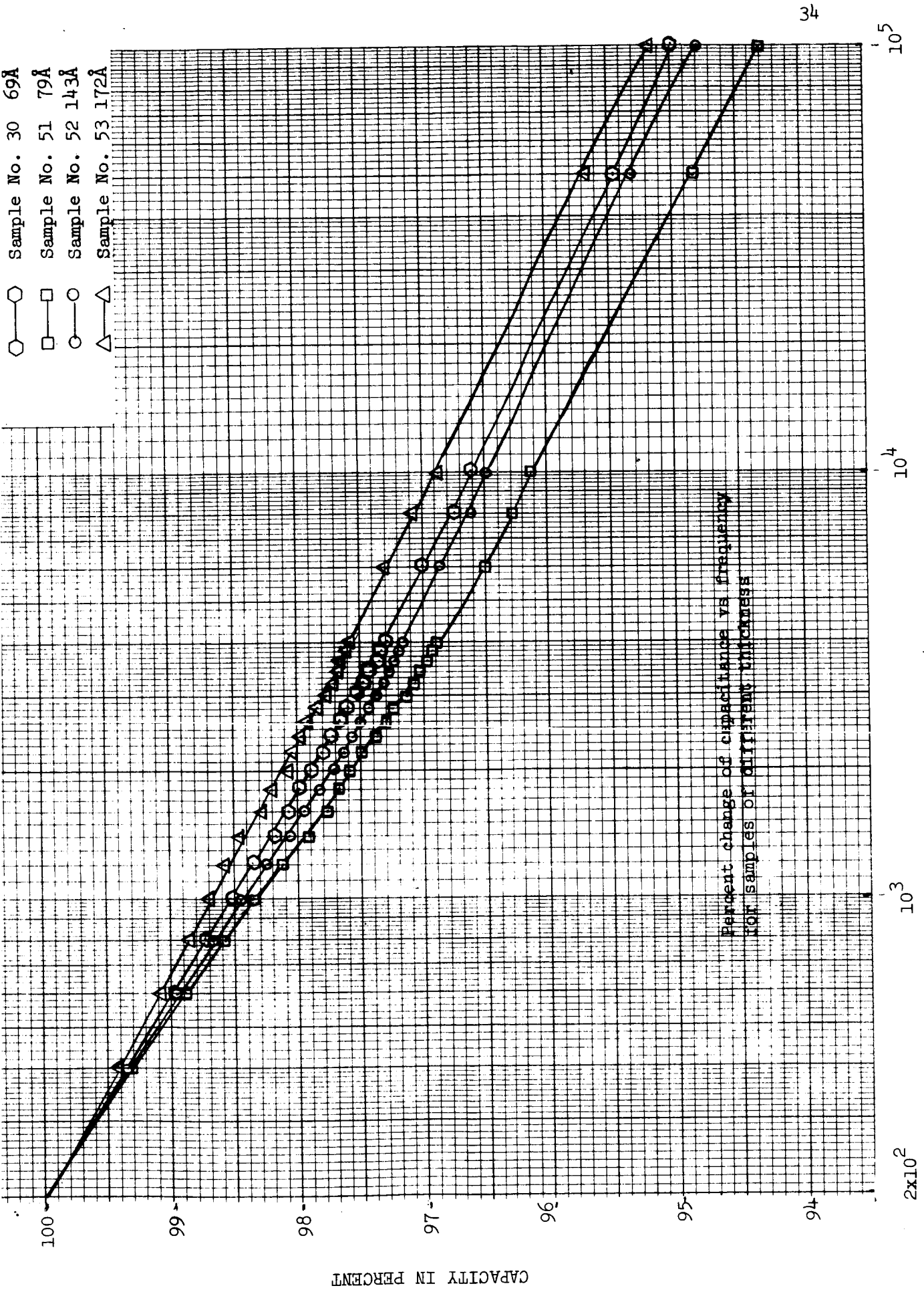


Figure 9

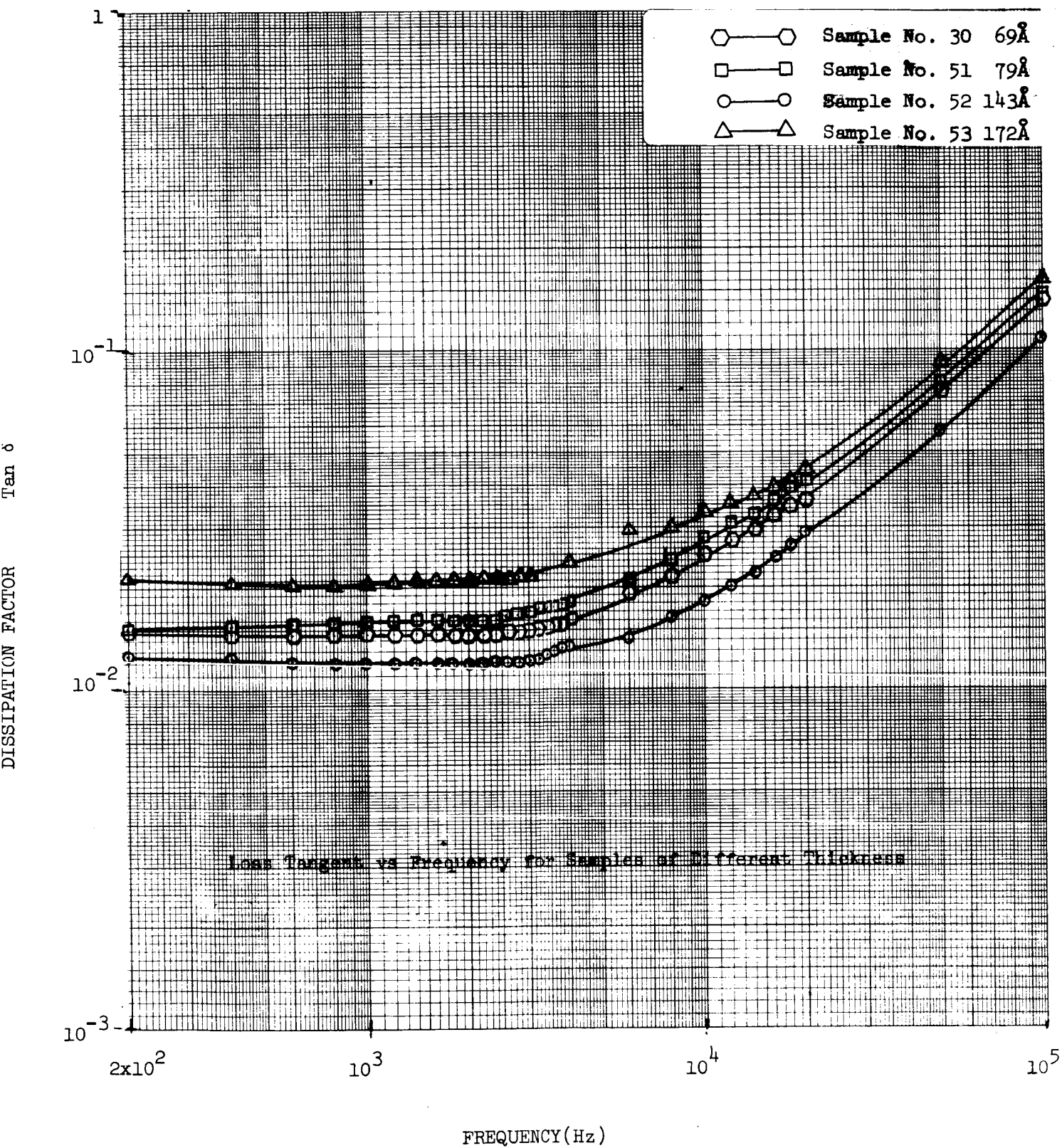
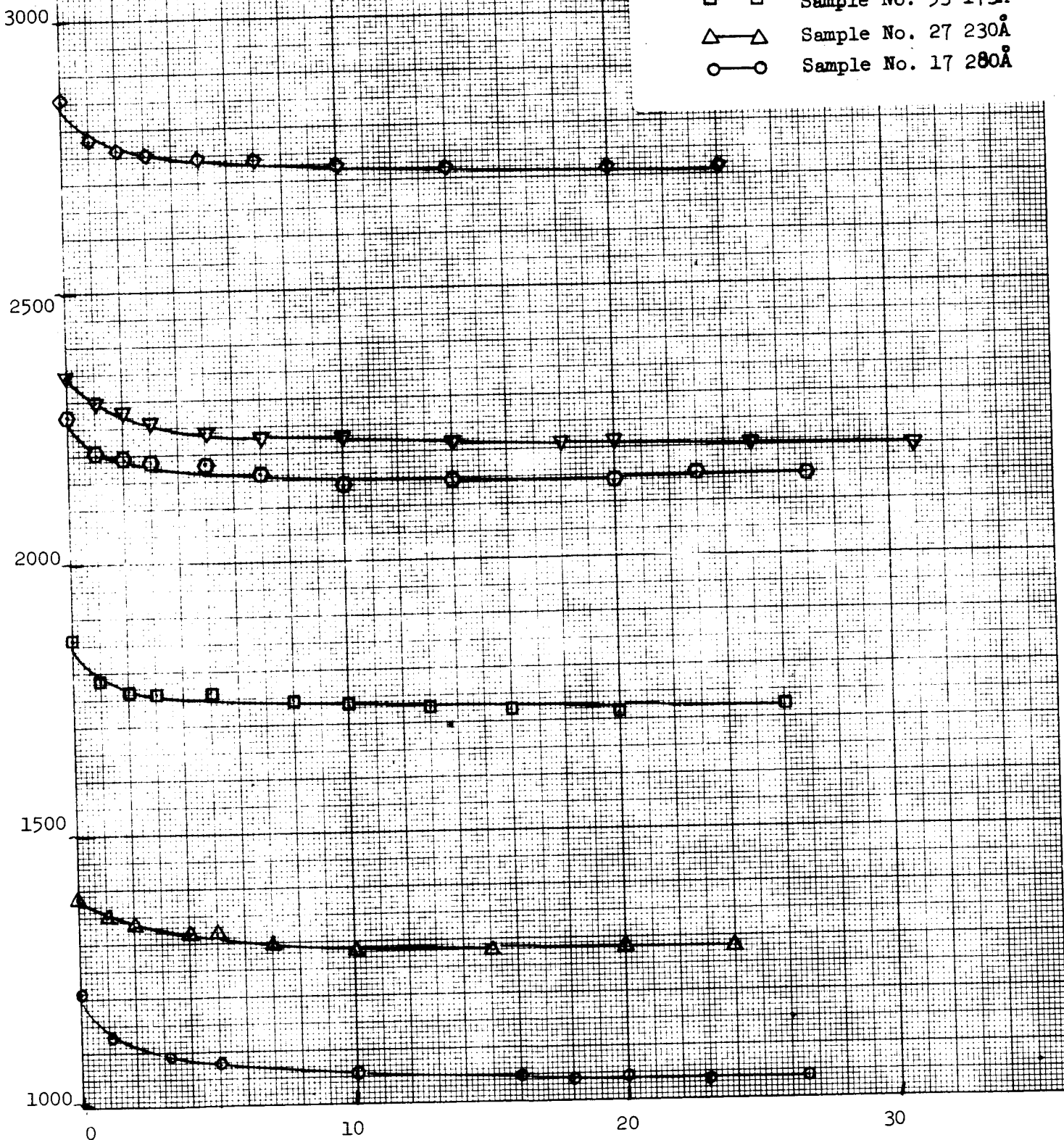


Figure 10

Capacitances vs time for samples of different
thickness at 1 KHz

- ◇—◇ Sample No. 20 112Å
- ▽—▽ Sample No. 14 137Å
- Sample No. 52 143Å
- Sample No. 53 173Å
- △—△ Sample No. 27 230Å
- Sample No. 17 280Å



Time in Days Figure 11

a. Capacitance vs Frequency

Figure 7 is typical of the capacity of MPM structures. The total change of a few percent from 200 Hz to 100 Hz with a break about 2-3Khz is common to all samples. The thickness of this particular sample is $143\overset{0}{\text{\AA}}$ as determined from the known area and dielectric constant and checked against the growing time.

b. Dissipation Factor vs Frequency

Figure 8 is the dissipation factor for the same sample showing an increase which becomes noticable about 3KHz and appears to have an increasing slope out to the limit of the range.

c. Percent Capacitance Change, Many Samples

Figure 9 is the capacitance change normalized as % Capacitance about 200Hz. Each curve is for a different thickness, but there is no systematic trend. This discourages hasty generalizations on separate surface and bulk effects, although it must be realized there is some uncertainty in the thickness as calculated. Separable surface and bulk effects cannot be said to be unresolvable at this point.

d. Dissipation Factor vs Frequency, Many Samples

Figure 10 again shows a consistent trend in the value of D with frequency. In all cases a constant value at low frequencies is established and an increase near 3KHz. The rising portion does not appear to have a straight-line asymptote which discourages a simple RC model.

C. AGING CHARACTERISTICS OF POLYMER DIELECTRICS

1. Description of Experiment

a. Aging Set-up

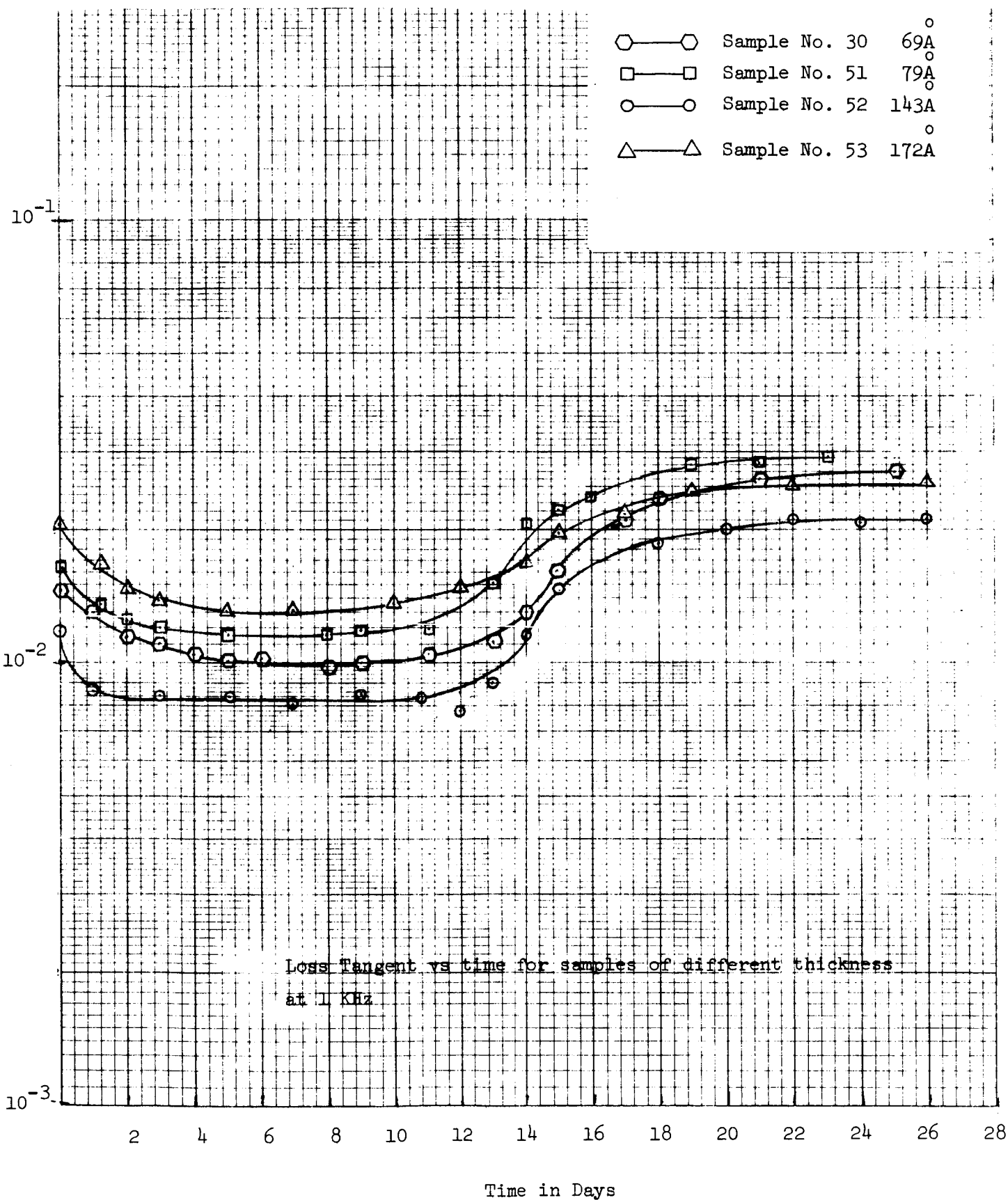


Figure 12

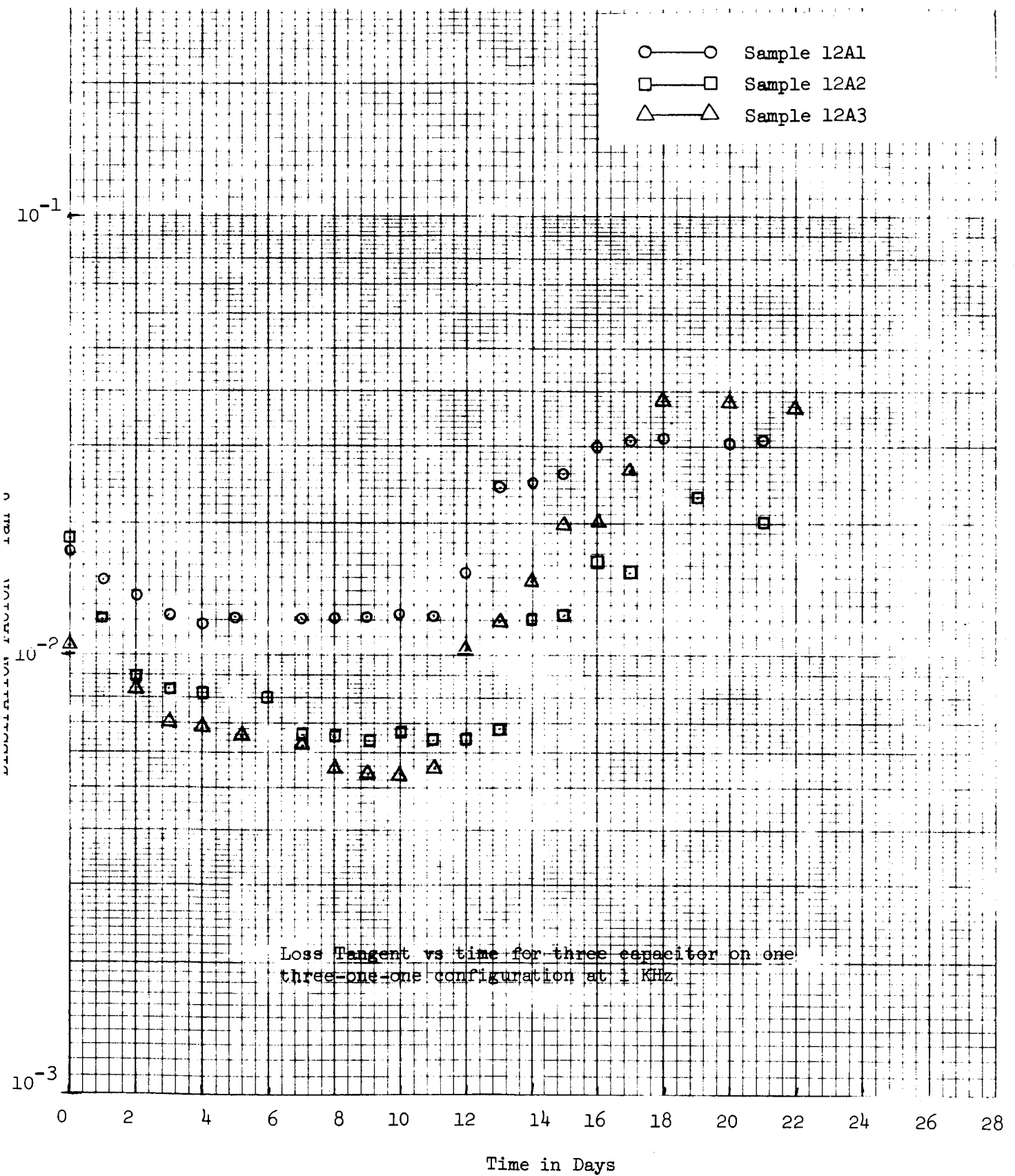


Figure 13

Samples to be aged are stored in air at room temperature in plastic boxes. Some have been stored in a 10 micron vacuum for several days and showed little tendency to age until removed to the air. Aging then proceeded as if it were a fresh sample. The separation of dry air and wet air effects and the measurement of aging rate with temperature are incomplete but will use a similar approach.

b. Measurement

The measurements are identical to those previously described, so the only variation reflected in the data is the effects of aging.

2. Experimental Results on Cross-Type Samples

a. Capacity vs Time

Figure 11 shows the capacity of several samples of thickness between 112 A and 280 A changed a few percent in a few days and leveled off.

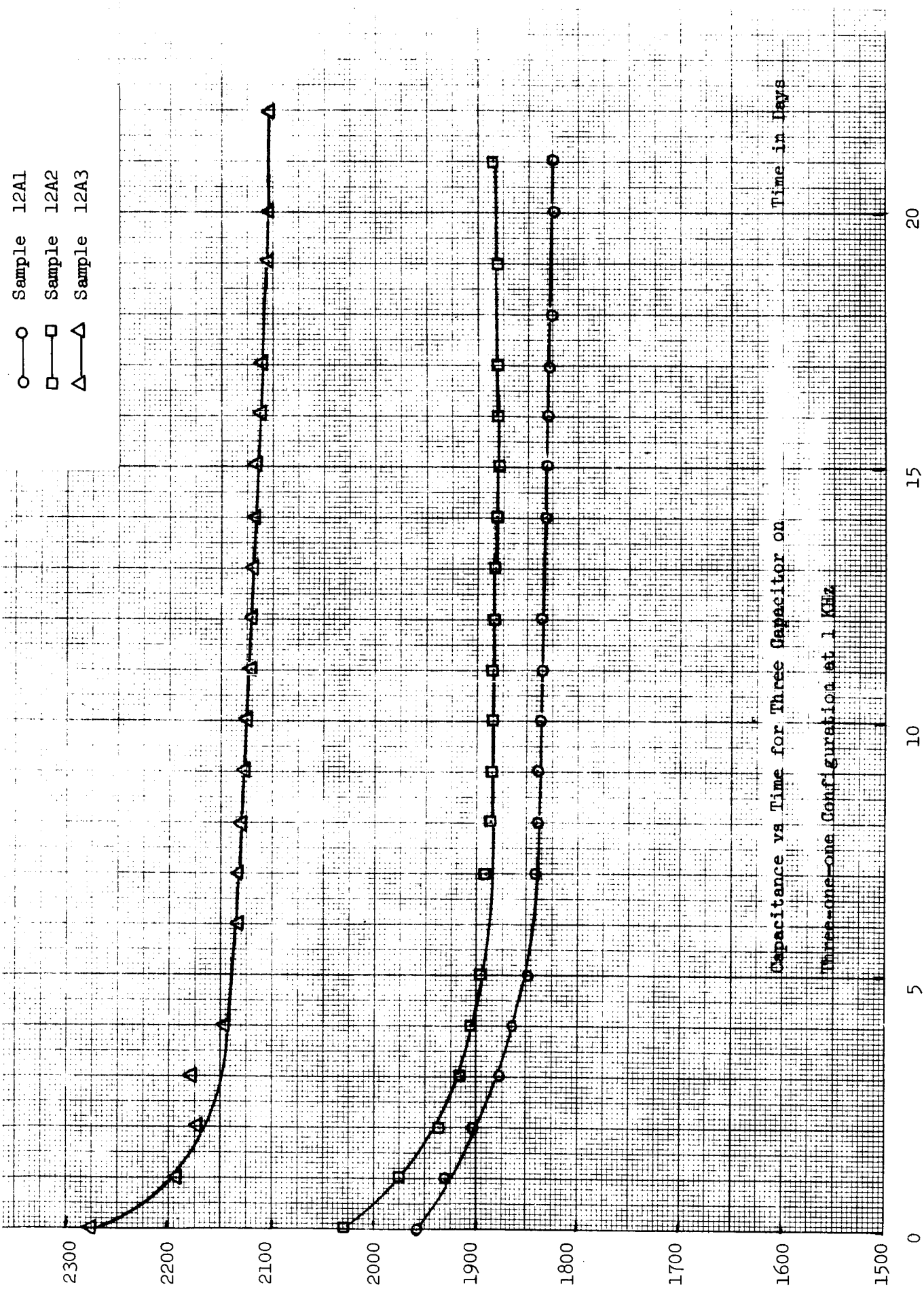
b. Dissipation Factor vs Time.

Figure 12 shows a uniform trend in all samples with an initial drop in 2-3 days, a level value until about 2 weeks had elapsed, then a rise over a period of a week then a level value after that. All dissipation factor and capacity vs time measurements were made at 1 KHz.

3. Experimental Results on Three-Dot Samples

a. Capacity vs Time

The three-dot configuration have an indistinguishable aging trend from the cross-type samples which is expected, but variations in total capacity between "identical" elements suggests some local variation in average thickness of the film. The data for Figure // shows a capacity spread of about 12%. This could be accounted for



Time in Days (Figure 14)

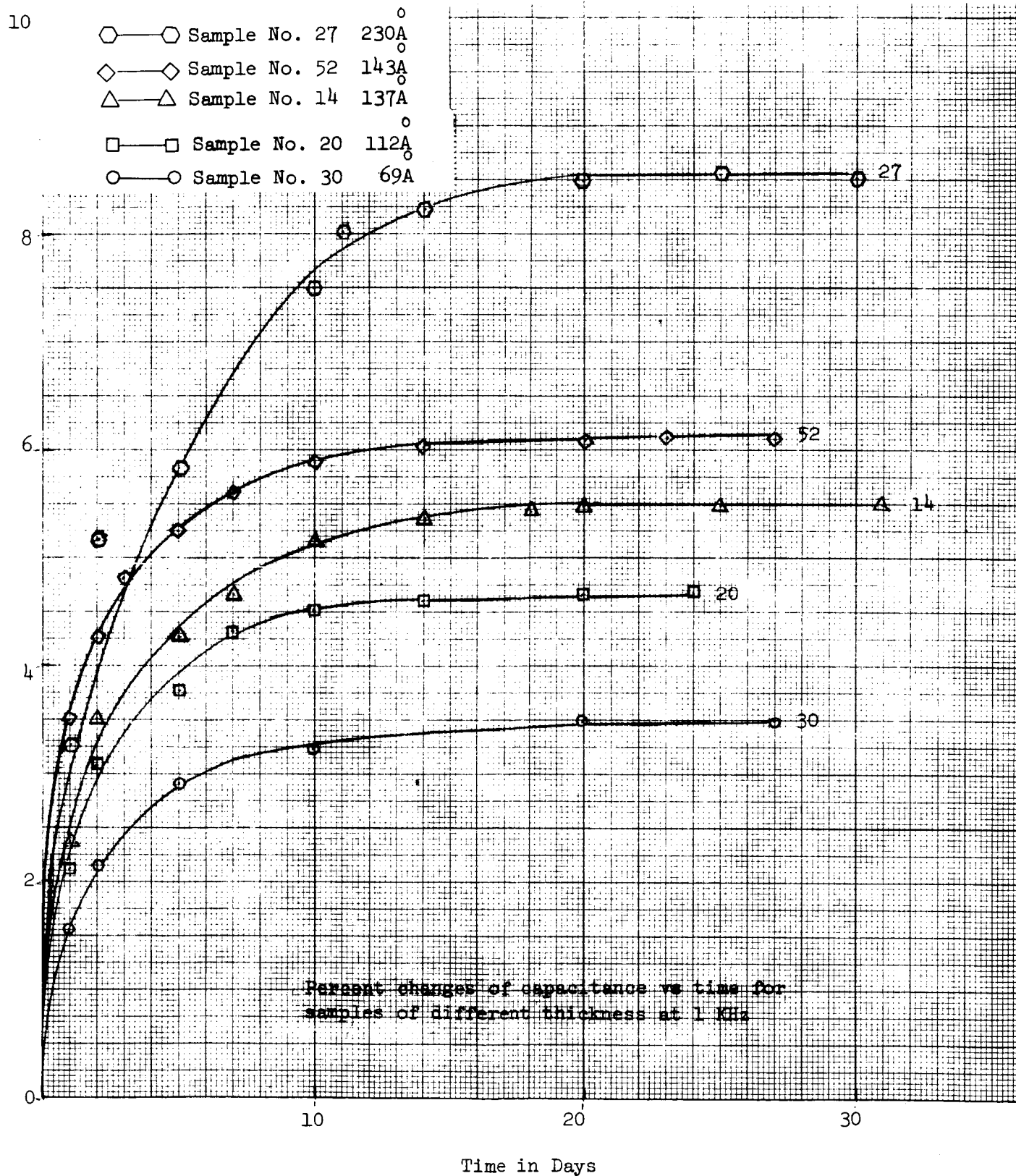


Figure 15

by a 6% spread in measuring the "diameter" of the dots, so does not completely resolve the question of thickness uniformity.

b. Dissipation Factor vs Time

Figure 13 shows the same behavior as Figure 12, an initial drop, a level value for nearly two weeks, then a rise to a final level value after about 3 weeks.

4. Percent Capacitance Change vs Thickness vs Time

Figures 14 and 15 show clearly the aging is, at least in part, a bulk effect. Figure 11 shows a systematic increase in the total capacity change for thicker samples. Figure 15 is a re-plot of Figure 11 which shows the aging process is essentially complete for all thickness up to 280 Å after 20 days. The thicker samples lag behind the thinner ones as shown by the drop in the curves for shorter periods of time.

D. ANALYSIS OF EXPERIMENTAL RESULTS

The polymer dielectric films have proven to be a very useful material for study of MIS thin film devices. A list of properties significant to the program is given below:

1. Films from 60 Å to 1000 Å in thickness can be grown with excellent control of growing rate. Thickness in this range can be obtained to within a few % of a desired value.
2. The films are free of pin-holes for non-replicating metals such as Aluminum.
3. The polymer ages in air to a stable dielectric after about three weeks.
4. Capacity changes of a few percent are typical for the aging period. The dissipation factor changes over a much wider range during the same period in a way that suggest more than one effect is present.

5. Percent capacity charge at 1 KHz for aged samples is proportional to thickness. This is a strange behavior but undoubtedly reflects some structural change in the polymer. More measurements are needed here.
6. Both capacity and dissipation factor are functions of frequency. The model suggested is a resistor-capacitor equivalent network in which the dissipation peaks at some frequency about 1 MHz. The apparent capacity has a component which decreases about 5% in the range of 200 Hz to 100 KHz, with a characteristic break at 3 KHz.
7. The dissipation factor is undoubtedly voltage dependent in view of the exponential increase in charge transport as a function of voltage. We observe that, whatever the charge transport mechanisms are, there is adequate current flow and dielectric strength to use this polymer in the study of field penetration into a semiconductor substrate.

The analysis of the polymer film is continuing to establish physical models, probably including a Debye relaxation mechanism in addition to the analysis in Vol. III of the First Annual Report.

V. OPTICAL DIGITAL TRANSDUCER CONCEPTS

The photodielectric effect in semiconductors is inherently digital since an optically-stimulated circuit reactance can control the frequency of resonance. In contrast, the photoconductive effect is inherently an analog response. The frequency change can readily be interpreted digitally while the conductivity change is primarily interpreted as a change in analog current or power level.

The photodielectric effect has been studied intensively in the Electronic Materials Research Laboratory under DOD and NASA sponsorship. At present a satisfactory theory has been derived to account for the behavior, which is a low-temperature effect. The effect is seen in two classes of electrodynamic behavior of photo-induced carriers; (1) free electron (and hole) inertia forces being interpreted as a capacitive component in a microwave field, and (2) trapping of electrons and holes in states which have increased polarization due to lower binding energy. The theory of the class (1) above was treated in Vol. II, pp 44-54 of the Annual Report and in Bibliography, items 91-98 of the same volume. Additional references are given in this report.^{1,2}

A. FREE ELECTRON MODEL

The free-electron model has

$$\delta\omega = \omega G \epsilon_1^{-2} \epsilon_\psi \quad (V-1)$$

where $\delta\omega/\omega$ is relative frequency change of a cavity containing the semiconductor sample, G is the filling factor, ϵ_1 is the lattice dielectric constant, and ϵ_ψ is the photodielectric shift in dielectric constant as given in Eq V-2.

$$\frac{\epsilon^*}{\epsilon_0} = (\epsilon_1 - \epsilon_\psi) - j \frac{\epsilon_\psi}{\omega_L \tau} \quad (V-2)$$

Here ϵ^*/ϵ_0 is the complex relative dielectric constant, $\omega_L = \omega(1 - \omega_p^2/\omega^2)$, τ is the

carrier momentum relaxation time, and the plasma frequency is given by $\omega_p = (ne^2/m^*\epsilon_o\epsilon_1)^{1/2}$ for thin cylindrical samples. The expression for ϵ_ψ becomes

$$\epsilon_\psi = \frac{e^2 (\omega_L/\omega) \tau^2}{m^* \epsilon_o \epsilon_1 (1 + \omega_L^2 \tau^2)} n_f \quad (V-3)$$

where n_f is the density of free carriers.

In materials like Si and Ge the free carrier density at 4.2°K is very small in the absence of light, typically 10^9 cm^{-3} or less, which means the plasma frequency is well below the frequency of measurement, typically 1GHz. Optical densities are proportional to lifetime and incident light power, with a total sensitivity of about 10KHz per milliwatt per cm^2 for a wafer 1 cm in diameter and 1 mm thick in the cavity configurations shown in Fig V-1.

Power absorption can be derived in terms of the absolute value P, or the relative value at a ratio P/P_o where P_o is the absolute power without illumination.

$$P_\psi = \frac{\epsilon \omega_o \epsilon_\psi E^2}{2\omega_L \tau} = \frac{\epsilon^2 E^2}{2m^* \epsilon_1^2} \frac{\tau}{1 + \omega_L^2 \tau^2} n_f \quad (V-4)$$

and

$$P_\psi/P_o = \frac{E_\psi^2}{E^2} \frac{\omega}{\omega_L} \frac{1 + \omega_{Lo}^2 \tau^2}{\omega_{po}^2 \tau^2} \epsilon_\psi \quad (V-5)$$

or

$$\frac{P_\psi}{P_o} = \frac{E_\psi^2}{E_o^2} \frac{\epsilon_1}{G} \frac{1 + \omega_{Lo}^2 \tau^2}{\omega_{po}^2 \tau^2} \frac{\delta \omega}{\omega_L} \quad (V-6)$$

where E is the sample electric field assuming negligible losses in the cavity, ω_{Lo} and ω_{po} are the zero light values of ω_L and ω_p respectively, and both n and P_o include thermal carrier density assumed independent of light intensity. Eq (V-6) is independent

of calibration errors associated with the optical source and provides clues to changes in E . This is useful because the optical absorption and diffusion processes in the sample require ω_p^2 to be distributed parameter which smears a simple fit of data and theory.

Figures V-2, V-3, and V-4 show the frequency change, dielectric constant change and plasma frequency growth, and calculated power absorption as a function of light intensity on Si along with observed data.

This is a true digital transducer in the form of a radiation detector. The bandwidth is several megacycles and both sensitivity and bandwidth can be controlled by selection of the semiconductor parameters. Optical wavelength is also subject to choice simply by selection of materials. For example InSb would have useful response at greater than 5 microns if the crystal is highly pure.

Application of such a detector would be in optical sensing such as infrared mapping. The scanning rate could be higher than with many photosensitive materials and a wide range of wavelengths would be available. Additional research will be needed to completely understand and catalog the materials which can be used in the free-carrier mode. An ideal set of materials would be those with graded bandgaps and recombination lifetimes which are controlled by trapping levels in optimum places in the bandgap.

B. TRAPPED-CARRIER MODEL

Class (2) behavior has been observed in cadmium sulphide and opens a different group of materials to investigation. In silver-doped cadmium sulphide (CdS:Ag) the bandgap is 2.58 eV and has a dominant hole trap state at 1.0 eV above E_v due to Cd vacancies, and an electron trap 0.35 eV below E_c . In addition there is distribution of shallower traps between the silver level, E_a , and the conduction band edge. At

4.2°K bandgap light (in the range 4800-6000 Å) has the overall effect of transferring electrons to the Ag level, and trapping holes at the Cd vacancy level E_q . Since recombination can no longer take place the result is a permanent, or photographic, change in crystal polarization, at least until the crystal is returned to a higher temperature. This class of behavior places materials at our disposal which have extremely long lifetimes, hence can be extremely sensitive. In principle the same behavior can be expected in other compounds semiconductors but at longer wavelengths. Figure V-5 shows the frequency change over a period of several hours with constant illumination.

The trapped carrier differential equation to a complex dielectric constant similar to Eq. (V-2)

$$\frac{\epsilon^*}{\epsilon_0} = \epsilon_r = \epsilon_{r0} + \Delta\epsilon_r = \epsilon_1 + \Delta\epsilon'_r - j\Delta\epsilon''_r \quad (V-7)$$

The change $\Delta\epsilon'_r$ is due to the change in polarization of electrons excited to traps at states with energy E_j , or

$$\Delta\epsilon'_r = \frac{\epsilon_1 + 2}{3} \frac{e^2}{m^*\epsilon_0} \sum_j \Delta n_j \frac{\omega_{oj}^2 - \omega^2}{(\omega_{oj}^2 - \omega^2)^2 + (\omega/\tau)^2} \quad (V-8)$$

where Δn_j is the increase of carrier density and ω_{oj} is the resonant frequency of the carrier in the trap. Since $\omega_0 \gg \omega$ we simplify to

$$\Delta\epsilon'_r = \frac{\epsilon_1 + 2}{3} \frac{e^2}{m^*\epsilon_0} \sum_j \frac{\Delta n_j}{\omega_{oj}^2} \quad (V-9)$$

and

$$\omega_{oj}^2 = \frac{2}{m^*} \frac{(4\pi\epsilon_0)^2}{e^4} (E_c - E_j)^3 \quad (V-10)$$

The summation over j includes all electron trapping states up to E_c which includes the dominant Ag level along with a distribution of defect and residual impurity states. When the traps fill, presumably from the deepest-lying states to those closest to E_c a circulation with the conduction band causes a rapid increase in photoconductivity. Figure V-6 reflects this by the photoconductivity data at 77°K for the same sample. The free carrier density is too small to be observed until over 20 minutes have elapsed and then the growth is very evident. At 4.2°K the same trend is expected displaced only in time.

C. PHOTODIELECTRIC DIGITAL TRANSDUCER

This phase of research has been a significant development since it suggests an immediate application to NASA programs in visible and infrared detectors. This work is completely new, with the first report of photodielectric effects in semiconductors made by Arndt and Hartwig. Subsequent work in this laboratory has brought the understanding to near maturity. A systematic search will be started to optimize material properties so there is a choice of wavelengths, sensitivities and response times for specific applications. Among other questions to be investigated is the range of temperatures over which the photodielectric effect could be used. The basic materials research is, hopefully, going to be funded more generously from separate sources. The development of digital transducers can then be part of the program under NGR-44-012-043.

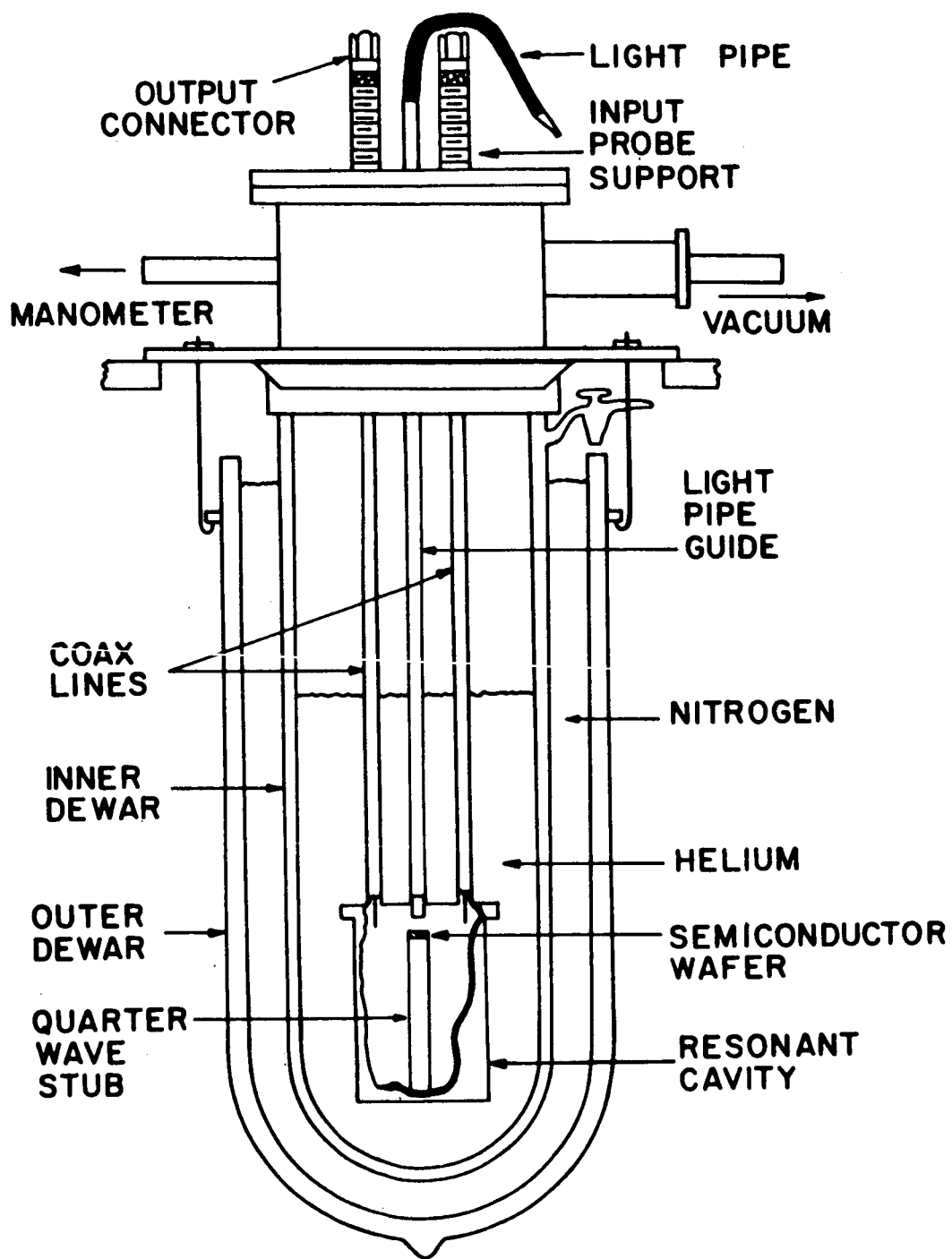


Fig. V-1

Cross Section of Superconducting Resonant Cavity
 Showing Position of Semiconductor Wafer

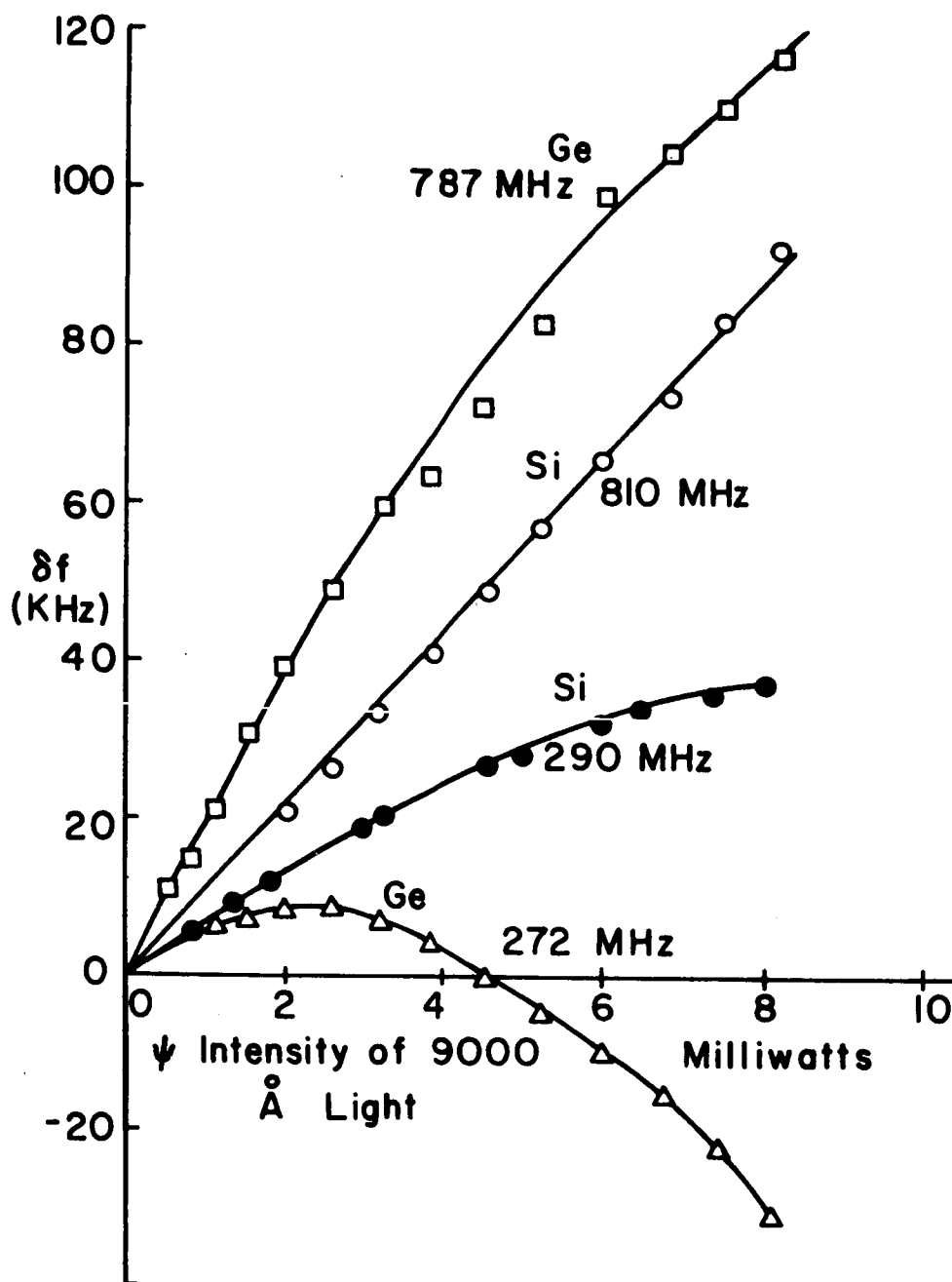


Fig. V-2

Frequency Change in KHz for a 525 ohm-cm N-Type Silicon Wafer at 290 MHz and 810 MHz, and a 60 ohm-cm P-Type Germanium Wafer at 272 MHz and 787 MHz at 4.2°K

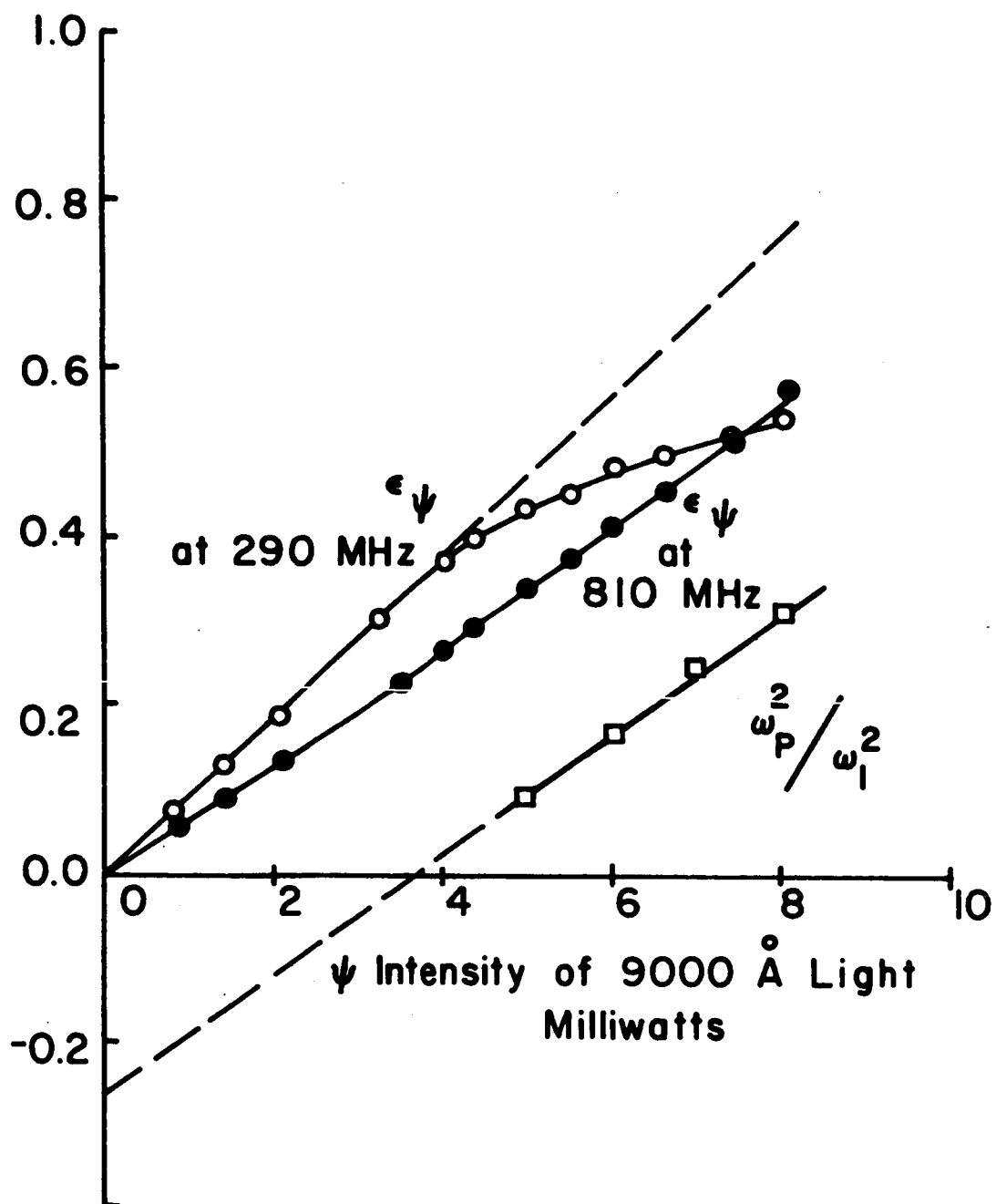


Fig. V-3

Change in the Real Part of the Complex Dielectric Constant of Silicon with 9000 Å Light Intensity, and the Corresponding Change in Relative Plasma Frequency with Respect to 290 MHz.

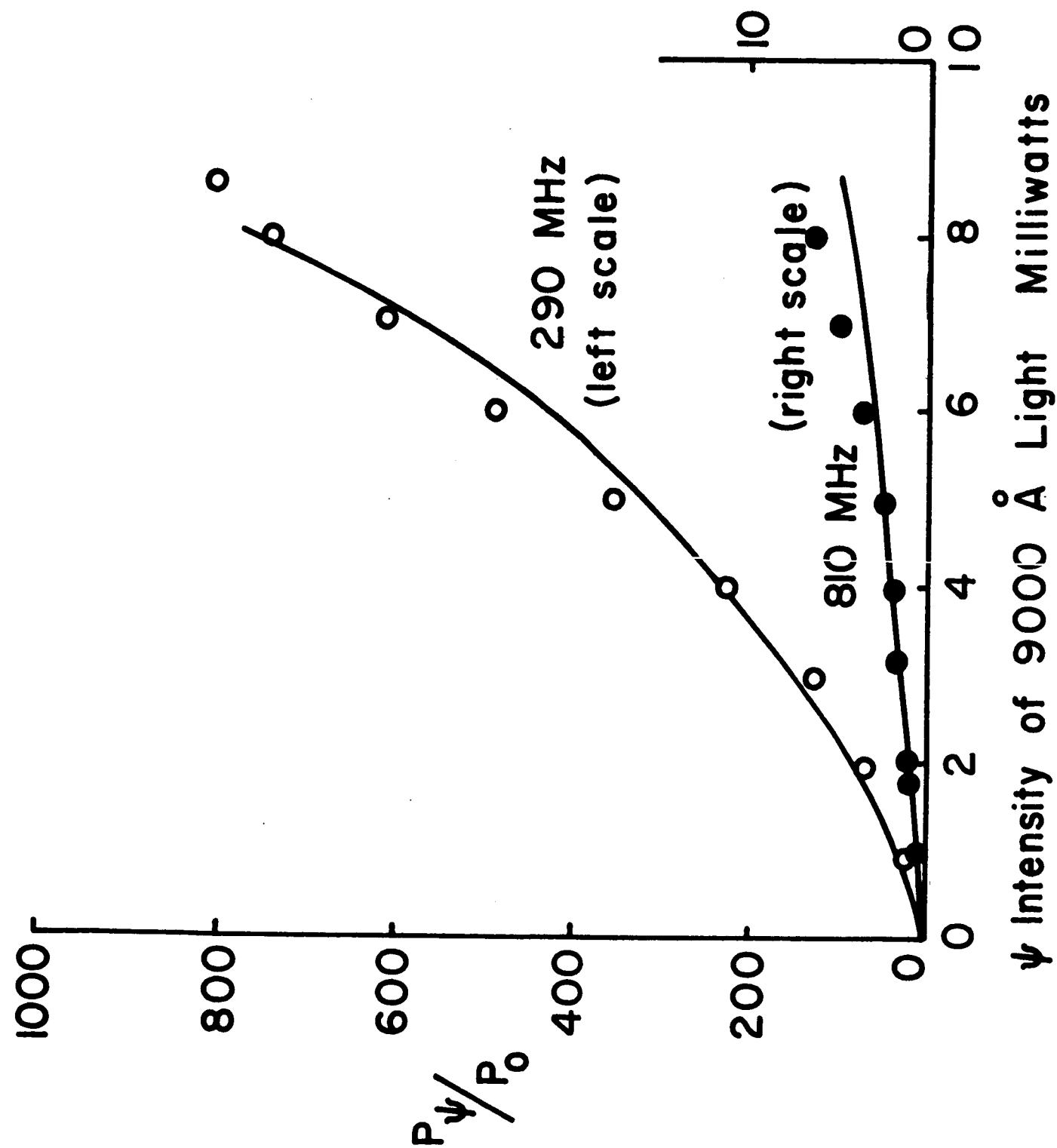


Fig V-4

Calculated Power Absorption as a Function of Light Intensity with Experimental Data Points for Silicon at 290 MHz and 810 MHz at 4.2°K. Theoretical Plasma Resonance at 290 MHz is at 10.4 Milliwatts of Illumination on the Wafer

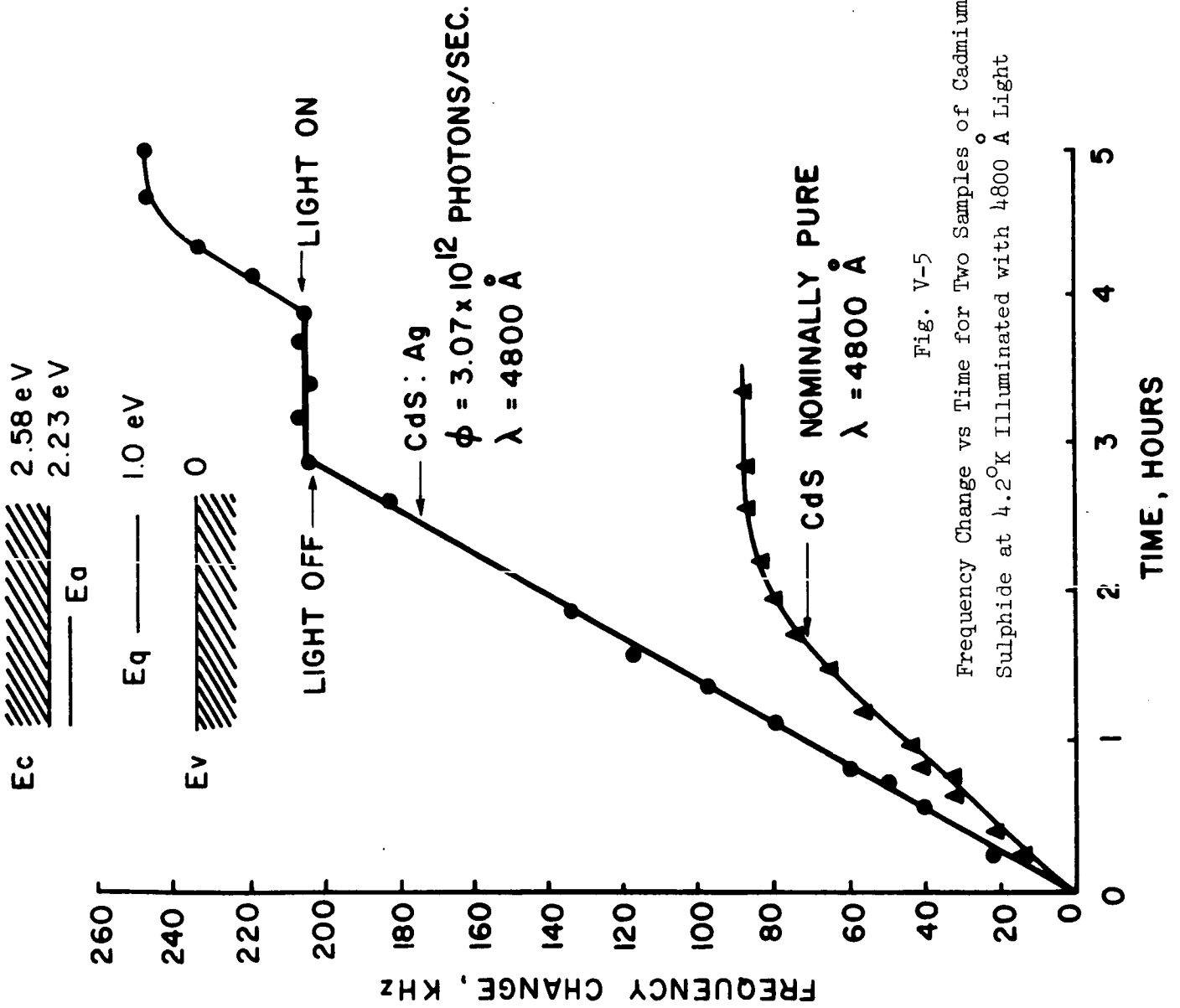


Fig. V-5
 Frequency Change vs Time for Two Samples of Cadmium
 Sulphide at 4.2°K Illuminated with 4800 Å Light

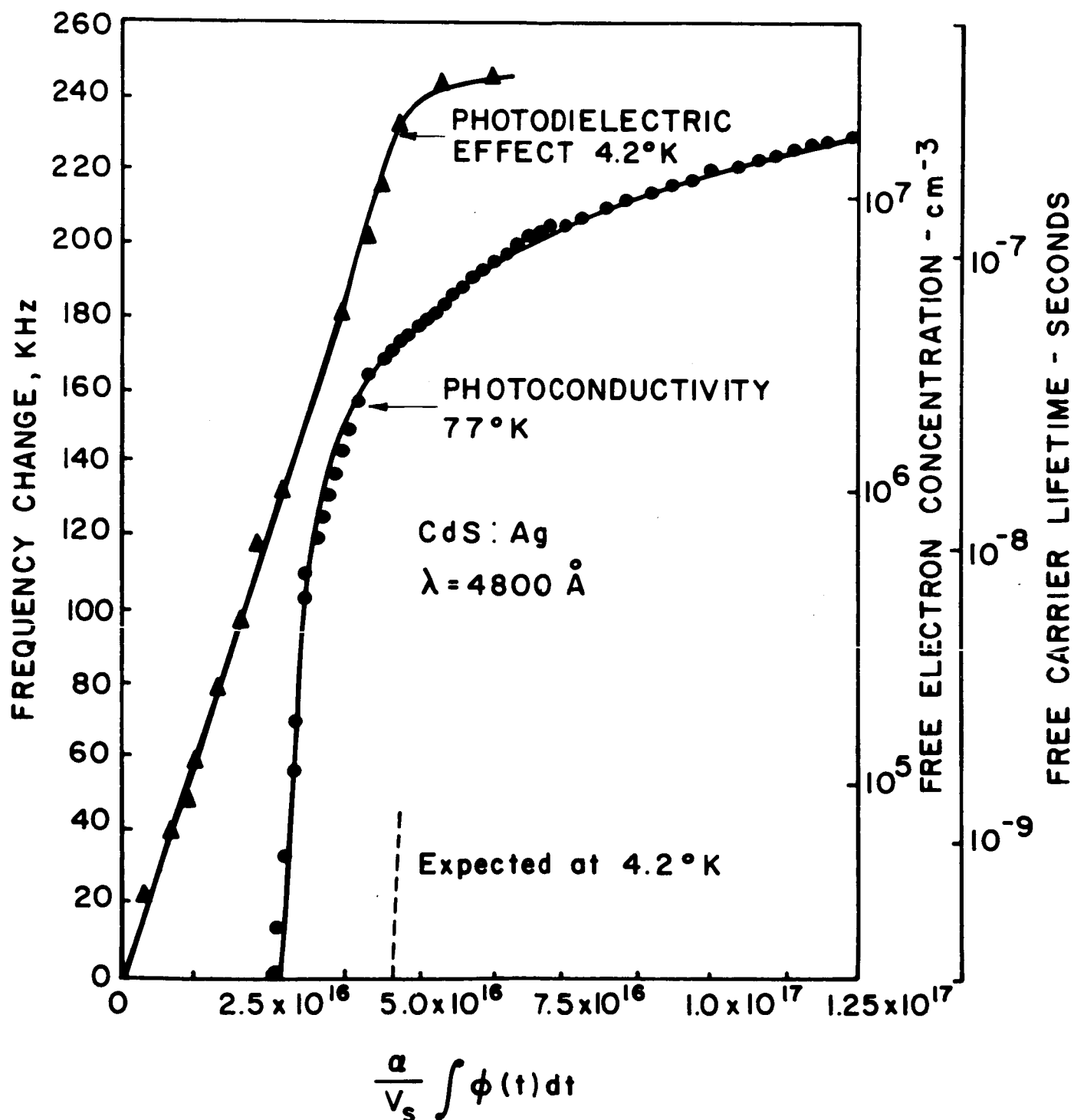


Fig. V-6

Comparison of Frequency Change at 4.2°K and Photoconductivity at 77°K vs Time with Constant 4800 Å Illumination. Free Carrier Concentration and Lifetime Scales Apply to Photoconductivity

VI. NEW DIGITAL DATA STORAGE PRINCIPLE

The subject of the grant, Research on Digital Transducer Principle, is concerned with generation of digital information.

During the past decade the field of information storage and retrieval has expanded at an enormous rate since these systems limit the overall capability of information processing in many important situations. More information is being stored and processed every year and the requirements for data storage in computer memories and library files have reached the limits of the present (conventional) systems. There exist a current need for memories of 10^9 - 10^{10} bits capacity and such large memories are vital for the important fields of pattern recognition and for artificial intelligence. The large capacity of these memories urgently requires a new method of extremely high density information storage. The most promising ones are using electron or laser beams for the information storage and retrieval which permits densities of 10^8 bits/cm².

A new member of the laboratory staff had been engaged during the past 2 1/2 years in demonstrating the feasibility of the magneto-optic memories with densities limited only by the wavelength of light. This effort was recently successfully concluded by him at the Jet Propulsion Laboratory under NASA sponsorship. He has demonstrated the feasibility of information storage densities of 10^8 bits/cm² using Curie-point writing and Faraday effect on MnBi thin films. This materials has certain drawbacks, including destruction temperature only 60°K above the Curie-point and extreme difficulties of epitaxial preparation. There exists a current need for better materials which are easier to prepare in order to advance the development of magneto-optic memories. The immediate need is for ferromagnetic materials of low optical losses, large Faraday rotation, large magnetic anisotropy with the easy axis

perpendicular to the plane of the film, and Curie Temperatures between 50 and 500°C. There is a large group of intermetallic compounds (consisting of transition metal elements combined with S, Se, Te, P, As, Sb, Bi, Si, and Ge) with known crystal structure of the NiAs (or other hexagonal) type, and consequently, large anisotropy if ferromagnetic. There is, however, little or nothing known about the magnetic and magneto-optic properties of these materials.

It is the purpose of his research program to study the thin-film preparation techniques, and the magnetic and magneto-optic properties of many of these materials with the ultimate goal of eventually being able to "custom tailor" the required properties for different applications, but selectively mixing or doping different starting materials.

Thin films of the constituent materials will be evaporated sequentially in vacuum of 10^{-6} torr on a substrate. The substrates will be chosen to permit epitaxial growth of the compound. Mica is the most promising material at the moment. After the sequential evaporation, the substrate will be heat-treated in vacuum (and magnetic field if necessary) to permit: (1) diffusion of the two starting materials into each other and (2) epitaxial crystal growth of the compound. The thickness of the finished films will be between 500 and 5000 Angstroms, depending on the optical losses. The preferred thickness is such that the optical transmission is between 10 and 30%. The films will be covered in vacuum with a thin protective passive layer (SiO or other inert materials) to prevent oxidation or moisture effects in ordinary atmosphere.

The observable optical properties of the films will be studied with a high-power polarized light microscope, measuring optical transmission, Faraday rotation, and observation of domain structure. The crystallographic properties will then be studied with available X-ray diffraction equipment. In addition, the magnetic anisotropy and Curie Temperature, as well as magneto-optical properties as

a function of temperature, will be studied with equipment to be built in-house.

It is expected that this program on digital transducers at The University of Texas and to respond to the need for better digital systems by NASA. Since this work is being done in close collaboration with all phases of the existing programs in the laboratory, we hope to assist where possible, at least until it becomes self-sufficient.

BIBLIOGRAPHY

1. Mayer, L., "Curie-Point Writing on Magnetic Films," J. Appl. Phys. Vol. 29,
p. 1003, 1958
2. Mayer, L., "Magnetic Writing With an Electron Beam," J. Appl. Phys., Vol. 29,
p. 1454, 1958
3. Chen, D., "Direct Observation of Domain-Wall Movements in MnBi Films,"
J. Appl. Phys., Vol 38, p. 1309, 1967.

VII. ATTENDANCE AT MEETINGS, PAPERS, AND PUBLICATIONS

A. MEETING

1. Conference between W.H. Hartwig and R.R. Richard at NASA Manned Spacecraft Center to review research progress October 24, 1967.
2. 1967 APPLIED SUPERCONDUCTIVITY CONFERENCE, Nov. 6-8, 1967, Sponsored by the College of Engineering at The University of Texas at Austin and the U. S. Atomic Energy Commission. Conference Chairman, W. H. Hartwig.

B. PAPERS

The three papers were read by personnel from the Electronic Materials Research Laboratory which will appear in the May, 1968 issue of the Journal of Applied Physics as a Special Issue. Abstracts are referenced below.^{3,4,5}

C. PUBLICATIONS

1. Jackie L. Stone and William H. Hartwig, "A Unique Laser Detector Utilizing the Photodielectric Effect in Cooled Semiconductors", Laboratories for Electronics and Related Sciences Research, Technical Report No. 39, The University of Texas at Austin, Sept 1, 1967.
2. J. C. Christian and H. L. Taylor, "Ionic Diffusion at the Aluminum-Aluminum Oxide Interface", J. App. Phys., Vol. 38, No. 10, Sept., 1967
3. J. M. Victor and W. H. Hartwig, "RF Losses in the Superconducting Penetration Depth", 1967 Applied Superconducting Conference Abstracts,
4. J. L. Stone and W. H. Hartwig, "Performance of Superconducting Oscillators and Filters", 1967 Applied Superconducting Conference Abstracts, pp. 96-97, The University of Texas at Austin.
5. G. D. Arndt, W. H. Hartwig, and J. L. Stone, "Photodielectric Detector Using a Superconducting Cavity", 1967 Applied Superconducting Conference Abstracts, pp. 94-95, The University of Texas at Austin
6. J. R. Yeargan and H. L. Taylor, "Conduction Properties of Pyrolytic Silicon Nitride Films", Journal of the Electrochemical Society, Vol. 115, No. 3, pp. 273-276, March, 1968. (Accepted for publication)